ML-TDR-64-56

# SUBSTRUCTURE AND MECHANICAL PROPERTIES
OF REFRACTORY METAL WIRES

56 p $3.00 hc
$0.50 mf

TECHNICAL DOCUMENTARY REPORT No. ML-TDR-64-56

MAY 1964

AF MATERIALS LABORATORY
RESEARCH AND TECHNOLOGY DIVISION
AIR FORCE SYSTEMS COMMAND
WRIGHT-PATTERSON AIR FORCE BASE, OHIO

Project No. 7351, Task No. 735101

D D C

JUL 27 1964

DDC-IRA   A

FOREWORD
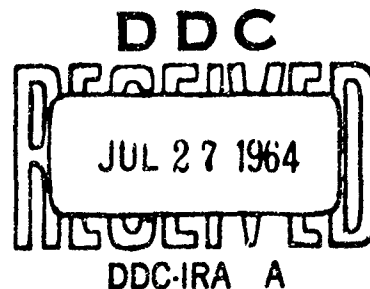
This report was prepared by the Massachusetts Institute of Technology, Cambridge, Massachusetts, under USAF Contract No. AF 33(657)-11238. This contract was initiated under Project No. 7351, "Metallic Materials," Task No. 735101, "Refractory Metals." The work was administered under the direction of the Air Force Materials Laboratory, Research and Technology Division with Lt. James E. Steedly, Jr. as project engineer.

The report covers the period April 1 through October 30, 1963.

ABSTRACT

Polycrystalline columbium wires of three levels of interstitial impurity content show steady work hardening in wire drawing to the highest strain obtained, a true strain of 5.1. This behavior contrasts to f.c.c. metals, which show saturation of work hardening at true strains greater than 2. During drawing of random-texture columbium, a fibrous microstructure and the [110] wire texture continually develop. If the material has an initial [110] texture, however, the texture diminishes because of deformation band formation, and subsequent recrystallization produces near-random orientation. Swaged wire also shows continued work hardening and develops a cylindrical texture at high strains.

Torsion stress-strain curves for both polycrystalline and single crystal columbium have been obtained and the effect of strain reversal studied. A region of work softening was observed in both as-drawn wire and single crystals after reversal of comparable forward strains in drawn wire annealed at 700°C or above prior to testing. The substructures produced during these experiments have been studied by electron microscopy and an attempt made to correlate the structure after forward straining with the extent of work softening. The results are discussed in terms of a jog-vacancy mechanism of work hardening.

This technical documentary report has been reviewed and is approved.

J. Perlmutter

F. PERLMUTTER
Chief, Physical Metallurgy Branch
Metals and Ceramics Division
Air Force Materials Laboratory

TABLE OF CONTENTS

ILLUSTRATIONS

ILLUSTRATIONS (CONT'D)

ILLUSTRATIONS (CONT'D)

1. General Introduction

The present investigation represents the continuation and extension of the work on fibering of refractory metals conducted as a portion of the program "Substructure and Mechanical Properties of Refractory Metals"[1-3].

At the end of the previous program[1], the experimental study of the relationship of microstructure, work hardening, and texture in the wire drawing and swaging of polycrystalline columbium was well advanced. The completion of this study constitutes Section 2 of this report. The results further support the previous conclusion that b.c.c. columbium shows steady work hardening to the highest strain produced by wire drawing, a true strain of 5.1. The concurrent transmission electron microscopy study of heavily drawn tungsten wire[1] has revealed dislocation arrays on (110) planes normal to the wire axis, which were interpreted as low-angle twist boundaries arising from twisting of the fiberlike grains in accommodating during heavy drawing to the shape changes of neighboring fibers. These dislocation arrays were considered to be a possible explanation for the steady work hardening at high strains, and suggested the study of work hardening and dislocation structures in torsionally deformed b.c.c. metals. This study was undertaken on columbium single crystals and polycrystals and the results are reported in Section 3. Typical of the complex nature of work hardening, no simple confirmations of the previous suggestions resulted, but the torsional strain hardening and accompanying dislocation structures have proved interesting in themselves.

1

2. Microstructure, Hardness, and Texture of Polycrystalline Columbium

2.1 Introduction

This section reports the completion of work previously undertaken under Wright Field contract and previously reported in part[1]. This report presents some additional experimental results and the conclusions reached.

This investigation correlates observations of microstructure, hardness, and texture of drawn and swaged columbium wires. Earlier results had indicated unusual microstructures and high work hardening at high strains during wire drawing[2-4], and suggested the need for systematic observations on wires of a single material.

2.2 Experimental Details

For completeness, the following description of the materials and treatments used is included. Other experimental techniques are the same as used before.

The three purities of columbium, Cb-50, Cb-150 and Cb-450, and one purity of nickel used in this work were initially wires 0.108 inches in diameter. When annealed at 2250° F, the 0.108 inch diameter Cb-150 and Cb-450 had a pronounced [110] texture, and the annealed 0.108 inch diameter Cb-50 had an approximately random texture. Table 1 gives the compositions of the materials.

TABLE 1

Composition and Source of Materials

Material	C	N	O	Source
	parts per million			
Cb-50		50		National Research Corp.
Cb-150	15	79	140	Wah Chang
Cb-450	--	--	628	National Research Corp.
	Ni percent	C	Other elements	
Nickel-270	99.97	0.005	traces	International Nickel Co.

The wires were drawn in twenty-one steps to 0.015 inch in diameter (reduction in area = 98 percent true strain = 3.8) and microstructural texture, and hardness data taken at various reduction steps. Later, the hardness of Cb-150 and Cb-450 was measured for reductions up to a true strain of 5.1 (reduction in area 98.7 percent). The observation that drawing the textured Cb-150 and Cb-450 to a 25 percent reduction and then annealing it produced a random texture made possible the production of 0.091 inch diameter wires of Cb-150 and 450 with random textures, which were then drawn to 0.015 inches in diameter (reduction in area = 97.8 percent, true strain = 3.5). Microstructural, texture, and hardness data were taken from these wires at various stages of reduction.

To obtain hardness data for a face-centered cubic metal with a relatively high melting point for comparison with the columbium data, the 0.108 inch diameter nickel was drawn to 98 percent reduction.

The textured 0.108 inch diameter Cb-450 was swaged in six steps to 0.034 inches in diameter (reduction in area = 90 percent, true strain = 2.3), and microstructural, texture, and hardness data were taken at various steps. Some of the drawn columbium wires were recrystallized, and hardness, grain size, and texture data obtained.

2.3 Results

2.3.1 Drawn Wires

The results on the microstructure, hardness, and texture of drawn columbium and nickel were previously reported[1]. In summary, the development of fibrous microstructures was observed, and the grains in columbium became ribbonlike in shape at high drawing strains. The hardness of all purities of columbium showed an initial rapid increase to true strains greater than 5. The hardness of drawn f.c.c. nickel approached a constant value at true strains greater than 2. Columbium wire with a strong initial [110] texture showed an initial randomization, attributed to the occurrence of deviating orientations in deformation bands, and then a gradual return of the [110] texture, particularly in the interior of the wire. Columbium wire with an initially random texture gradually developed a [110] texture, again particularly in the interior of the wire.

2.3.2 Recrystallization

a. Hardness and Grain Size

Hardness and grain size data were obtained from Cb-50 and Cb-450 recrystallized after drawing various amounts. The hardness (DPH) and the grain size data of Cb-450 recrystallized after drawing to reductions of up to 82 percent (true strain = 1.7), and Cb-50 recrystallized after drawing to reductions of up

3

to 98 percent (true strain = 3.8) are plotted as a function of the true strain prior to recrystallization in Figure 1. The grain size decreases as the amount of prior deformation increases. The hardness initially decreases as the amount of prior deformation increases, then becomes level. The level stage begins at a true strain of 2.5 in Cb-50, and at a true strain of 0.8 in Cb-450. The hardness decreases as the grain size decreases.

    b. Texture

        The material used in this work was received in the "as-worked" condition with the exception of Cb-50. The exact processing history of the Cb-150 and Cb-450 is unknown. However, they were worked down from a 3-1/2 inch diameter bar to 1/8 inch in diameter by processes including drawing. When these as-received materials were annealed, a pronounced [110] texture was obtained. The Cb-50 was received in the annealed form, and had an approximately random texture.

        The Cb-50 recrystallized after drawing to reductions up to 98 percent (true strain = 3.8) from an initially random texture exhibits the textures shown in Figure 2, which are all essentially random, except at the final stages, where in the outer third of the wire radius there is an increase in the intensity of the center diffraction arc, and in the inner third of the wire radius there is a decrease in the intensity of the center diffraction arc.

        Cb-450 was drawn to a reduction in area of 81 percent (true strain = 1.7) from an initial [110] recrystallization texture, and samples at each stage of reduction were recrystallized. Also, a sample of this material was recrystallized after drawing to a reduction of 98 percent (true strain = 3.8). At the second stage of reduction (reduction in area = 25 percent, true strain = 0.3) the recrystallization texture became essentially random, and remained random through the 81 percent reduction stage, as shown in Figure 3. No data at 3/4 or 1/4 of the original drawn wire diameter were taken up to this point. At 98 percent reduction in area, a complete series of diffraction patterns was obtained, and the bottom horizontal row in Figure 3 shows that a [110] recrystallization texture was obtained.

        A sample of Cb-150 was recrystallized after drawing to a reduction of 98 percent, from an initially textured wire, and is similar to the recrystallized Cb-450 at the same reduction in Figure 3. Cb-150 and Cb-450 drawn from initially random textured material (obtained by recrystallizing 0.108 inch diameter annealed material drawn to 25 percent reduction in area) were recrystallized at higher reduction stages. The textures obtained were similar; an example is shown in Figure 4 for Cb-150. The highest reduction here, 97.8 percent (true strain = 3.5), was not as much as in the previously discussed cases, and while there is a slight texture

4

formed in the last reduction step, it is not as distinct as those in prior experiments.

2.3.3 Swaged Wires

Cb-450 was swaged in six steps to a reduction of 90 percent (true strain = 2.3) from material with a pronounced [110] texture. The microstructure, texture, and hardness at each stage of reduction were determined.

a. Microstructure

The microstructures were presented in the previous report[1], and they are similar to the earlier results [2-4] in showing the "spiral nebula" structure at high reductions.

b. Texture

Figure 5, a 110 diffraction ring composite of the swaged Cb-450 shows that the initial [110] annealing texture is destroyed in the core at the same stage that grains are shown by microscopic examination to be severely deformed. The texture does not reform in the core, even at the final reduction (true strain = 2.3, reduction in area = 90 percent). The exterior shell of the wire tends to retain the initial [110] texture, even in the smallest wire. When the spiral nebula structure appears, the cylindrical texture[5] appears in the exterior shell, as shown by the diminished intensity of the central diffraction arc.

c. Hardness

Figure 6 is plot of the hardness of the swaged Cb-450 versus true strain, and shows the initially sharp hardness increase at higher strains. There are not enough data points to indicate whether or not there is a tendency for the hardness to level off after the initial increase. The variation of hardness across the diameter of each specimen is small for the as-annealed and the 29 percent reduction in area (true strain = 0.35) specimens, and increases sharply in the 46 percent reduction (true strain = 0.6) and all smaller specimens. A bell shaped curve for the hardness traverse across each individual specimen is found in the latter wires, the hardness at the center being 30 to 40 diamond pyramid hardness numbers greater than that at the edge.

2.4 Discussion of Results

2.4.1 Recrystallization

The appearance of deformation bands has been shown to be the structural feature that is responsible for the destruction of an initial texture during drawing. The appearance of a random

annealing texture in wire drawn 25 percent reduction from material
with an initial [110] annealing texture coincides with the appear-
ance in the microstructure of deformation bands. Walter and
Koch[6] find that the recrystallization nuclei in a rolled iron-
silicon crystal are the dislocation cells that connect misoriented
adjacent deformation bands. In this case, only certain cells grew,
and a recrystallization texture was formed. In other cases, the
growth of many cells of different orientations seems possible.
Thus, in drawn columbium the boundaries between the deformation
bands are probably cells, which may furnish the many orientations
of nuclei required for a random recrystallization texture.

The grain size of recrystallized columbium, shown in
Figure 1, reaches a lower limit instead of decreasing further as
the amount of deformation prior to recrystallization is increased.
This could be due to an upper limit for the number of recrystal-
lization nuclei with increasing deformation, impingement of growing
nuclei, or grain growth. Impingement will cause a variation in
the grain size, which will lead to grain growth. The wires drawn
the most should recrystallize first, and thus have more time for
grain growth. The drop in hardness at high prior reductions and
small grain size is contrary to the usually accepted relation of
grain size and hardness. However, it is consistent with a grain
growth process occurring at high prior reductions, since this
would enable the dislocations to approach closer to an equilibrium
distribution.

2.4.2 Swaged Wires

The original texture was destroyed in the core by
swaging, as shown in Figure 5. This correlates with the micro-
structural observation that the grains in the core are indistin-
guishable.

When the spiral nebula structure appears, the cylindrical
texture appears in the exterior shell of the wire. This is to be
expected from the microstructure, since the grains are elongated
parallel to the wire surface, as well as in the direction parallel
to the wire axis. Thus, the deformation is locally similar to
rolling, and the {100} plane that tends to be parallel to the
rolling surface should be parallel to the swaged wire surface.
The {100} tends to be parallel to the surface in rolled body-
centered cubic metals, since elongation parallel to a <110> allows
a shape change in a <100> only, and compression is easier if a
<100> is parallel to the axis of compression.

The high hardness of the center of swaged wires (30 to
40 DPH greater than the edge) correlates with the highly dis-
turbed structure in the core of the wire.

6

2.5 Conclusions

The main conclusions of this investigation, including the work previously reported[1], are as follows:

2.5.1

As previously proposed[2,4], the origin of the curved grains in transverse section of heavily drawn wires of b.c.c. metals is directly related to the development of a [110] texture.

2.5.2

The destruction during drawing of the strong [110] annealing texture of columbium wires results from the formation of deformation bands, which rotate part of a grain away from the original orientation of the matrix.

2.5.3

Annealed columbium wire with an initial [110] fiber texture achieves a random texture after wire drawing approximately 25 to 75% reduction followed by recrystallization annealing. This is attributed to the presence of recrystallization nuclei of all orientations present in deformation band boundaries.

2.5.4

The cylindrical texture of b.c.c. wires results from swaging and is absent in drawn wires. The cylindrical texture is prominent in the outer portions of heavily swaged wires, when the spiral nebula microstructure is observed in transverse section.

2.5.5

Columbium wires of all interstitial purities studied undergo continued work hardening in drawing to the highest true strain produced, 5.1. This work hardening appears to be characteristic of b.c.c. metals, whether drawn or rolled. Nickel wires show saturation of work hardening at true strains greater than 2. This behavior is common in f.c.c. metals and suggests basically different work hardening characteristics at high strains compared to b.c.c. metals. Some instances of continued work hardening in f.c.c. metals at high strains may be a consequence of the effects of alloy or precipitation strengthening in addition to work hardening.

3. Microstructure and Asymmetric Strain Hardening of Poly-
   crystalline and Single Crystal Columbium

3.1 Introduction

Work hardening is a commonly used method for strength-
ening metallic materials. It has therefore been the subject of
numerous experimental investigations and theoretical discussions.
In this particular study, the asymmetric nature of work hardening
in columbium has been investigated.

A uni-directional working process produces an aniso-
tropic microscopic defect structure and, if the material is
polycrystalline, also modifies the grain morphology and crystal-
lographic texture. The strengthening resulting from such a
process is therefore anisotropic on a macroscopic scale. A
material which is sufficiently pre-strained in one direction
will exhibit a subsequent stress-strain relationship which is
asymmetric about the zero stress axis[7].

Torsional straining, which has been used in this
investigation, is well suited to a study of the asymmetry since
large strains and strain reversals are easily achieved with
relatively simple apparatus.

3.2 Experimental Techniques

Torsion tests were carried out in both single crystal
and polycrystalline material. The single crystals were in the
form of zone-refined 3.5 mm diameter cylindrical ingots. A
typical analysis is given in Table II.

Table II

Typical Analysis of Single Crystals

Element	Content, P.P.M.
C	<5
O	120
N	70
Fe,Cu	<1
Mo	10
Ta	100-1000

Orientation relative to a unit triangle are shown in Figure 7.
Polycrystalline material was in the form of heavily drawn 3.6 mm
diameter Cb-150 wire, with a total interstitial content of
approximately 235 p.p.m.

8

3.2.1 Electron Microscopy Specimens

Thin foils were prepared from the specimens by cutting a transverse section 2 mm in thickness, masking the curved surface with lucite, and chemically thinning in the apparatus shown diagramatically in Figure 8. Single crystals were thinned in a 30% HF (48%), 70% HNO_3 (70%) mixture; polycrystals were thinned in a 50% H_2O, 35% HNO_3 (70%), 15% HF (48%) mixture. At the first appearance of a hole, the specimens were removed and washed in distilled water then examined in a Siemens Elmiskop I operated at 100Kv.

3.2.2 Torsiometer

Torque-twist curves were obtained using the torsiometer shown in Figure 9. One end of the specimen was twisted at a constant 0.25 r.p.m. by means of a reversible, geared, synchronous motor. A lever clamped to the other grip and held between two compressed coil springs was used to measure torque. The lever deflection was less than 30' at the maximum torque recorded. This load cell was calibrated in both directions by suspending weights from the lever at a known distance on either side of the rotation axis. Deflections were measured either with a dial gauge or a differential transformer coupled to a Tinius-Olsen amplifier and recorder. Runs on comparable specimens using either method yielded reproducible results, but the differential transformer was found to be more convenient. Of the stress-strain curves reproduced in this report only the one in Figure 38 was obtained using the dial gauge.

The gauge lengths of the torsion specimens were produced by hand filing down to 1.95 mm diameter while rotating the specimen in a jig so as to obtain a parallel and uniform section. They were then etched down to about 1.80 mm in order to remove as much surface work damage as possible without destroying the uniformity of the cylindrical section. The final dimensions of each specimen were measured before testing.

3.3 Results

3.3.1 Single Crystals

Structures observed in the single crystal specimens before straining are shown in Figures 10, 11, 12, 13, 20 and 21. Of these, the latter two are typical of most of the area examined. Between 5 and 10 transverse sections of each unstrained crystal were prepared and an estimated 0.02 mm^2 of each of these was sufficiently thin for examination.

Figure 10 shows segments of dislocations in a {111} oriented foil which are bowed out by some stress within the foil.

9

These are apparently pinned or held back by some feature such as precipitate particles or vacancy jogs.

Figure 11 shows a dense tangle within a {123} oriented foil. These were uncommon and may be associated with an inclusion. Figure 12 shows a number of screw dislocations in a {110} oriented foil, which could be moved in a microscope by increasing the beam current above the usual operating value of 2-5 μA. Slip traces at top and bottom surfaces of the foil demonstrate the very wavy nature of slip at the ambient temperature in the microscope, which is presumably less than 100°C.

Figure 13 is of a {111} oriented foil and shows a type of double contrast seen occasionally in all orientations. A completely satisfactory explanation of these contrasts has not yet been found, but similar effects have been shown to be due to coherency strains around precipitates[8].

The stress-strain curves for single crystal specimens are shown in Figures 14 to 17. These curves were computed from the recorded data using (angle of twist)(specimen radius)/(gauge length) as a measure of shear strain. In order to correlate the defect structure with various stages of the deformation process, the straining of certain of the crystals was halted at specific points on the stress-strain curve and thin foils for electron microscopy were prepared.

Figure 18 is a combined plot of representative stress-strain curves for all four of the investigated orientations. A yield drop of the type and magnitude shown in Figure 14 for the [110] specimen was occasionally seen in specimens of the other orientations. In cases where it was not observed, it may have been destroyed by handling operations, especially since the initial yielding of a torsion specimen occurs at the surface. The average work hardening rate of the low index crystals increases in the order: [110], [111], [100]. The work hardening rate of [123] crystals at large strains is very small although it is initially as high as that of [100] crystals. One specimen of this orientation was twisted through 12 revolutions without fracture occurring, during which the surface developed a uniform spiral ridge as shown in Figure 19.

On immediate reversal of the strain direction a pronounced Bauschinger effect [9] was observed in all of these crystals and, in fact, yielding occurred close to the zero stress axis. The initial rate of work hardening in the reverse direction is very high, particularly for the [111] and [100] crystals. The rate decreases rapidly, however, and becomes negative for the [100], [110] and [123] crystals. This is a radical departure from the classical Bauschinger effect[9] in which the work hardening rate approaches its value for an equivalent strain in the forward direction.

Sections were cut from specimens at the extreme stages of these curves and typical structures are shown in Figures 20-31. The plastic strain within a solid torsion specimen varies in a nonlinear way across a cross section.. These areas examined were all close to the centers of the torsion specimens, but because of the uncertainty regarding the exact position of the thin area only a qualitative relationship between strain and structure can be obtained.

After a forward strain of about 0.5 to 0.7, the photomicrographs show cellular structures which are fairly well defined in [100] crystals, less so in [111] crystals, and poorly developed in [110] crystals. In the case of the [100] crystal, the cell structure was elongated in the direction of the specimen axis as can be seen from the longitudinal section. The tendency to form a well-defined cell structure therefore appears to correlate with increasing work hardening rate for the low index crystals.

The cell structure in [123] crystals is quite well developed and may well have been formed during the initial stage of high work hardening. It should also be noted that the density of isolated dislocations is smaller, the greater the tendency to form well-defined cells.

Figures 28, 29, 30 and 31 show the microstructure of the specimens after strain reversal. The general effect of the strain reversal, as can be seen by comparison with the preceding figures, is a further definition of the cellular structure accompanied by a lessening of the isolated dislocation density within the cells. In [123] crystals, however, the tendency is for the cell walls to disperse.

3.3.2 Cold-Worked Polycrystals

Electron micrographs of the as-drawn wire are shown in Figures 32 and 33. As would be expected, the subgrains are very elongated and have a tendency toward an elliptical or elongated cross section. Selected area diffraction showed a large amount of misorientation between these subgrains, apparently of the order of 5-10°.

Annealing the cold-worked wires for two hours at 900°C resulted in the structure shown in Figure 34. Comparison with the structure of the cold-worked wires indicates that the very well-defined subgrain structure is largely removed while the density of more or less isolated dislocations is actually increased. The torsional strain applied in these experiments was small in comparison to the initial strain and had no visible effect on the substructure even for the annealed specimen after either forward or reversed straining.

Stress-strain curves for the as-drawn polycrystalline material are shown in Figures 35, 36 and 37. This material also shows a marked Bauschinger effect on reversing the strain direction. After a forward strain of greater than 0.15, the curve in the reverse direction shows a work hardening rate which decreases to a value less than that at the end of forward straining becoming distinctly negative in one region. The entire specimen undergoes some strain in the reverse direction until the peak of the stress-strain curve is reached. A cylindrical region, which we call a "twist" band, is then nucleated, presumably at a stress concentration, at the edges of which the torsional strain is discontinuous. Once nucleated the band grows towards both ends of the specimen, filling approximately half the length at zero net strain and the entire length at a negative strain equal in magnitude to the original positive strain. The sequence in forming this region is shown in Figure 39. Figures 40 and 41 are photographs of the band after etching the specimen in a 30% HF (48%), 70% HNO_3 (70%) mixture. The very elongated grain boundaries act as markers. The band front is frequently complex as shown in Figure 41. Several narrow bands form ahead of the front and eventually merge together as straining continues.

3.3.3 Annealed Polycrystals

Specimens annealed for two hours at 300 and 500°C prior to testing also formed bands of this type during reversed straining. However, a 2-hour anneal at 700°C or above removed this behavior. Figure 38 is the stress-strain curve for a specimen annealed at 700°C. It can be seen that although the work hardening rate becomes very small in the reverse direction no region of work softening was observed for forward strains which led to that effect in cold-worked specimens. The effect of annealing on the amount of forward strain necessary to cause band formation or on the magnitude of the strain discontinuity has not been investigated.

3.4 Discussion

The number of [111] directions which make the smallest angle with the applied shear stress is 2 for [110] crystals, 3 for [111] crystals and 4 for [100] crystals. The number of systems most readily operated therefore correlates well with the forward strain work hardening rate and the apparently concurrent tendency towards formation of a cellular structure in these low index crystals.

The majority of the theories of work hardening so far proposed have been based on the shape and strain-rate dependence of the progressive tensile stress-strain curve. The effect of reversing the stress direction has not generally been used as a criterion of the validity of a particular theory though a qualitative explanation of the Bauschinger effect has often been made[10].

Orowan has pointed out[7] that annealing of cold-worked material below the recrystallization temperature does not completely remove the Bauschinger effect. Those theories of work hardening which rely on the back-stresses associated with pile-ups or other dislocation groupings cannot be used to explain all of the observed Bauschinger effect. In the case of the Taylor model, for example, dislocations would leave the crystal on stress reversal and the behavior would be as shown in Figure 42.

The structures observed here by electron microscopy are consistent with a jog-vacancy mechanism of hardening[11]. Vacancy jogs move non-conservatively and hinder dislocation motion much more effectively than do interstitial jogs. Consider a dislocation within a tangled cell wall as shown in Figure 43. After forward straining, as a result of intersections with the forest, the dislocation has a large number of vacancies such as a, and we will postulate a smaller number of interstitial jogs such as b. On stress reversal jogs b become vacancy jogs and because of their smaller number yield occurs at a reduced stress. In fact, yield at virtually zero reverse stress might be expected because of the internal elastic strains that must be associated with such a cell wall. While the dislocation is detaching itself from the tangle, it will acquire a rapidly increasing number of vacancy jogs by intersections and the rate of hardening is high. Once in the cell interior, however, few intersections occur and the rate of strain hardening is approximately zero until tangling with the adjacent cell wall occurs and the flow stress again increases.

The stress-strain curves of cold-worked polycrystalline material are qualitatively similar to those of the single crystal specimens. Though it is possible that the similarity is not due to an identical hardening mechanism, it is notable that the microstructure of these specimens is more like those of the single crystals than the annealed polycrystals. From the electron micrographs it may be noted that the number of intersections a dislocation would undergo in crossing a cell or subgrain is small for both heavily cold worked single crystals and polycrystals, but is large for annealed polycrystalline material because of the large number of dislocations remaining within the grains. The qualitative nature of the strain reversal behavior may therefore be explained in terms of the above model.

References

1. B. L. Lement, D. A. Thomas, S. Weissmann, W. S. Owen and P. B. Hirsch; "Substructure and Mechanical Properties of Refractory Metals," ASD-TR-61-181, Part III (April, 1963), pages 107-121.

2. B. S. Lement, D. A. Thomas, S. Weissmann, W. S. Owen and P. B. Hirsch, "Substructure and Mechanical Properties of Refractory Metals," WADD-TR-61-181 (August, 1961).

3. B. S. Lement, D. A. Thomas, S. Weissmann, W. S. Owen and P. B. Hirsch, "Substructure and Mechanical Properties of Refra tory Metals," WADD-TR-61-181, Part II (October, 1962).

4. J. F. Peck and D. A. Thomas, "A Study of Fibrous Tungsten and Iron," Trans. AIME 221, 1240 (1961).

5. S. Leber, "Cylindrical Textures in Tungsten and Other Body-centered Cubic Metals," Trans. ASM 53, 697 (1961).

6. J. L. Walter and E. F. Koch, "Electron Microscope Study of the Structures of Cold Rolled and Annealed (100) [001] Crystals of High Purity Silicon-Iron," Acta Met. 10, 1059 (1962).

7. E. Orowan, "Causes and Effects of Internal Stresses," in Symposium on Internal Stresses and Fatigue in Metals, Detroit, 1958, Elsevier Publishing Company.

8. M. F. Ashby and L. M. Brown, "Diffraction Contrast from Coherency Strains," in Fifth International Congress for Electron Microscopy, Academic Press, New York, 1962.

9. R. L. Woolley, "The Bauschinger Effect in Some F.C.C. and B.C.C. Metals," Phil. Mag. 44, 597 (1953).

10. C. Zener, Elasticity and Anelasticity of Metals, The University of Chicago Press, 1948.

11. N. F. Mott, "Work Hardening of Metals," Trans. AIME 218, 962 (1960).
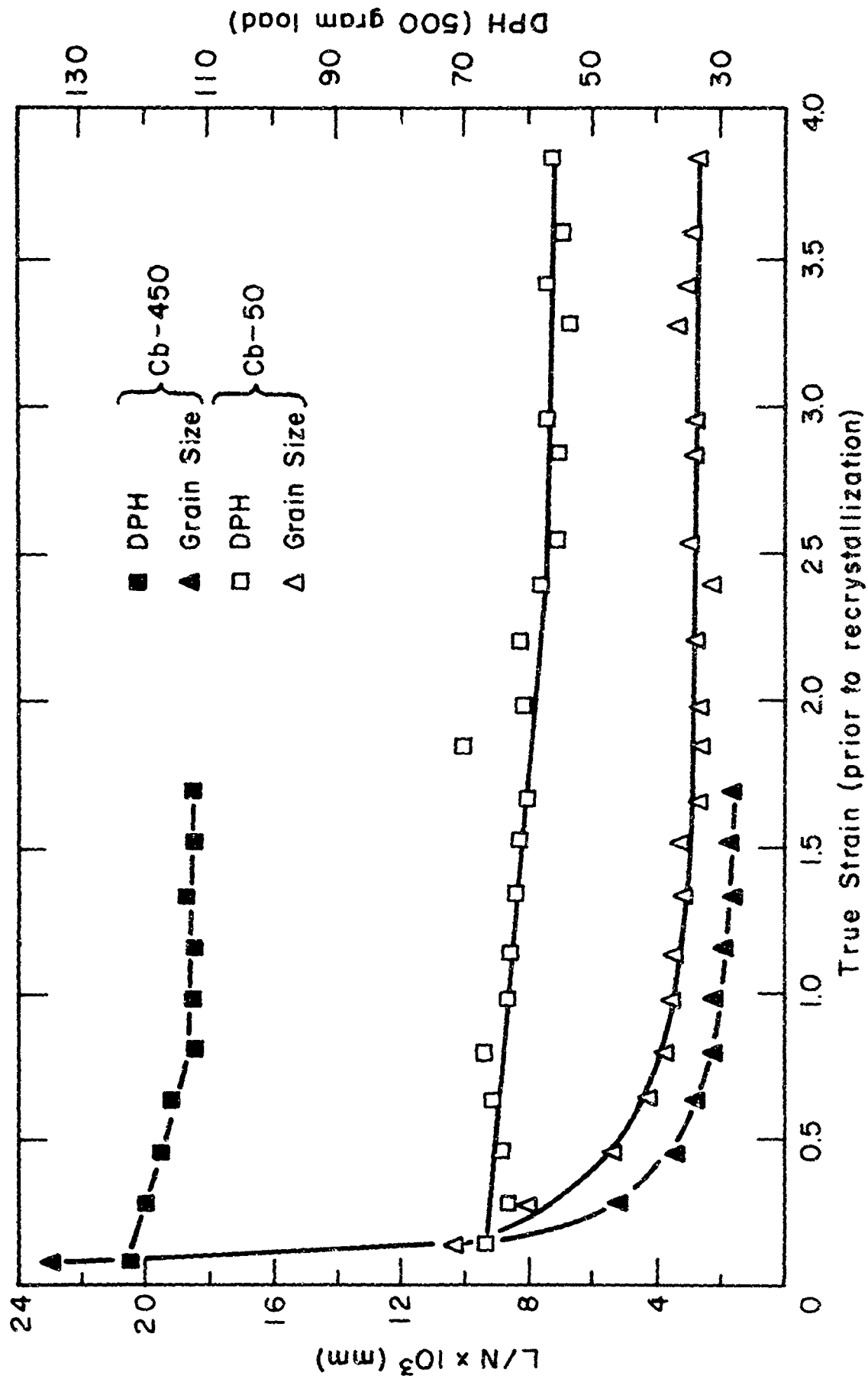
Fig. 1 Microhardness and grain size of drawn and recrystallized columbium wire

				TS	RA
				0.1	11%
				0.3	25%
				0.5	37%
				0.6	47%
				0.?	55%
				1.2	69%
				1.5	78%
				1.9	84%
				2.2	89%
				2.5	92%
				3.0	95%
				3.4	97%
				3.8	98%
1/1	3/4	1/2	1/4		
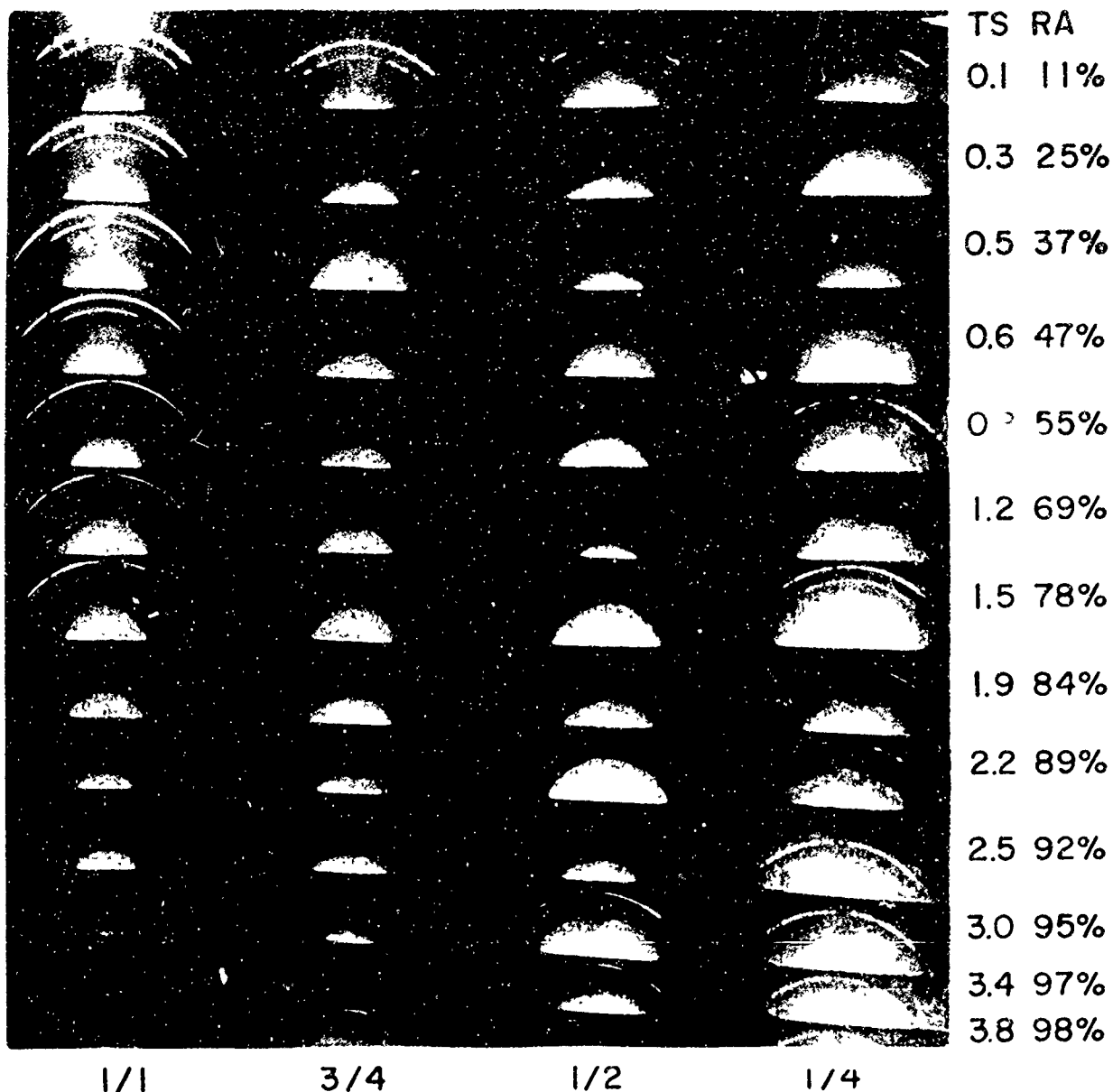
(Vertical columns show 110 diffraction rings of wire annealed and then examined as annealed and after chemical milling to 3/4, 1/2 and 1/4 diameter. Horizontal rows are labelled by the appropriate true strain (TS) and percent reduction in area (RA).)

Fig. 2 110 diffraction ring composite, Cb–50 recrystallized after drawing from random initial texture

	TS	RA
	0.1	11%
	0.3	25%
	0.5	37%
	0.6	47%
	0.8	55%
	1.0	63%
	1.2	69%
	1.3	74%
	1.5	78%
	1.7	82%
	3.8	98%

1/1   3/4   1/2
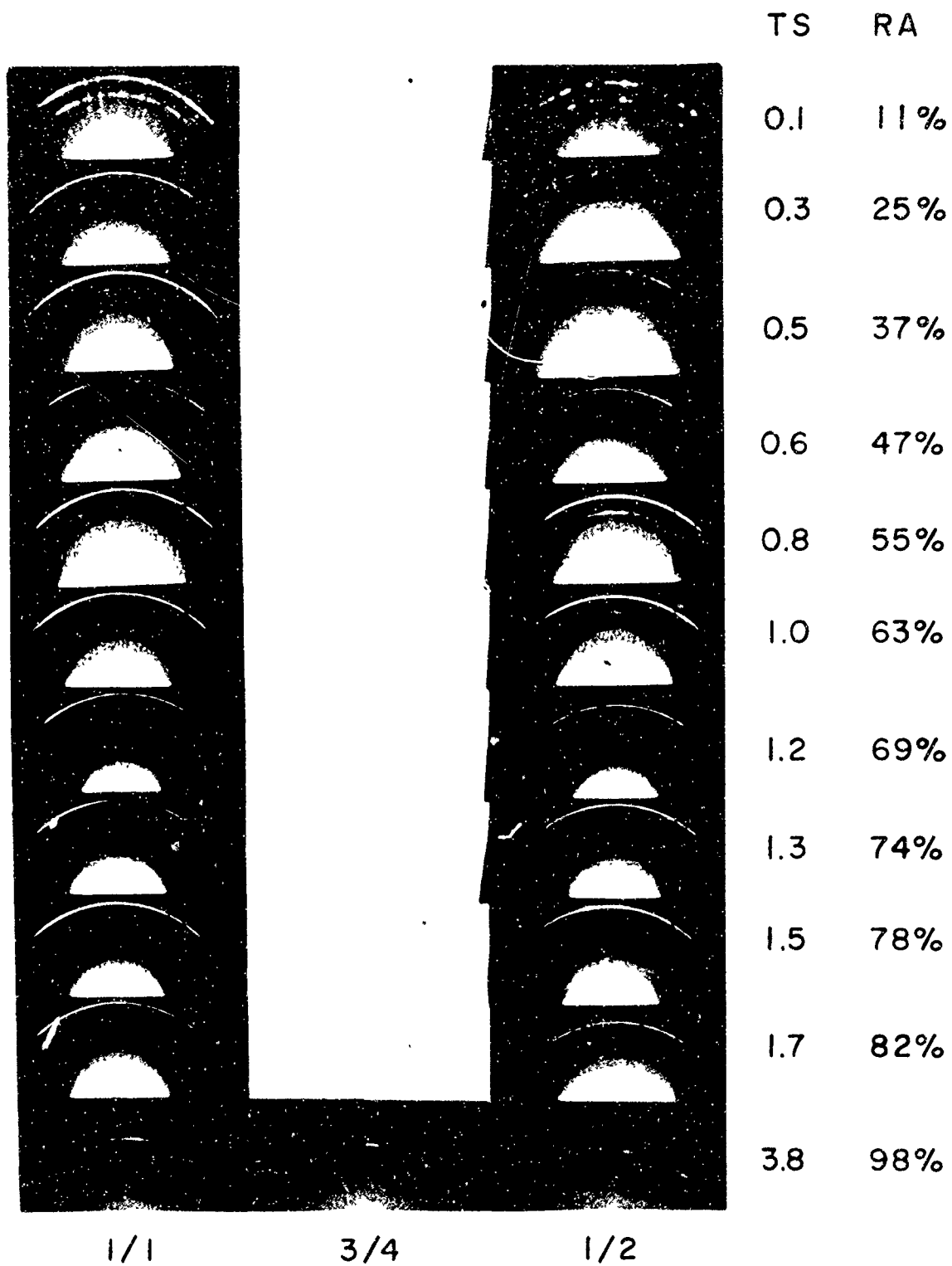
Fig. 3 110 diffraction ring composite of Cb-450, recrys-
tallized after drawing from $[110]$ initial texture

TS	RA
2.0	86%
2.2	88%
3.1	95%
3.5	97.8%

1/1   3/4   1/2   1/4
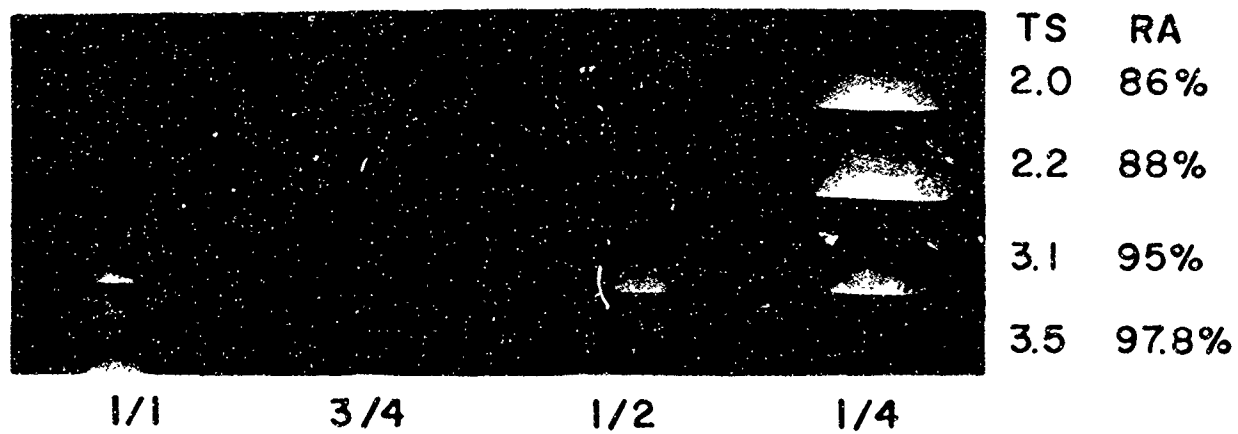
Fig. 4 110 diffraction ring composite of Cb-150, recrys-
tallized after drawing from random initial texture

TS	RA
0	0 %
0.35	29%
0.6	46%
1.1	66%
1.5	78%
1.9	84%
2.3	90%

1/1   3/4   1/2   1/4
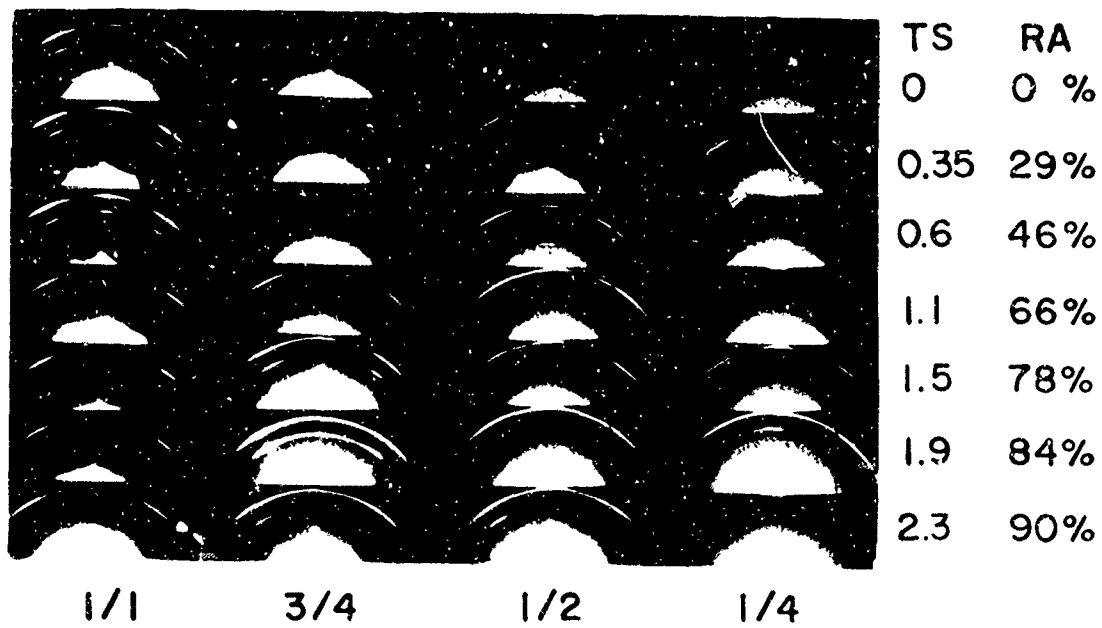
Fig. 5 110 diffraction ring composite, swaged Cb-450,
[110] initial texture

18
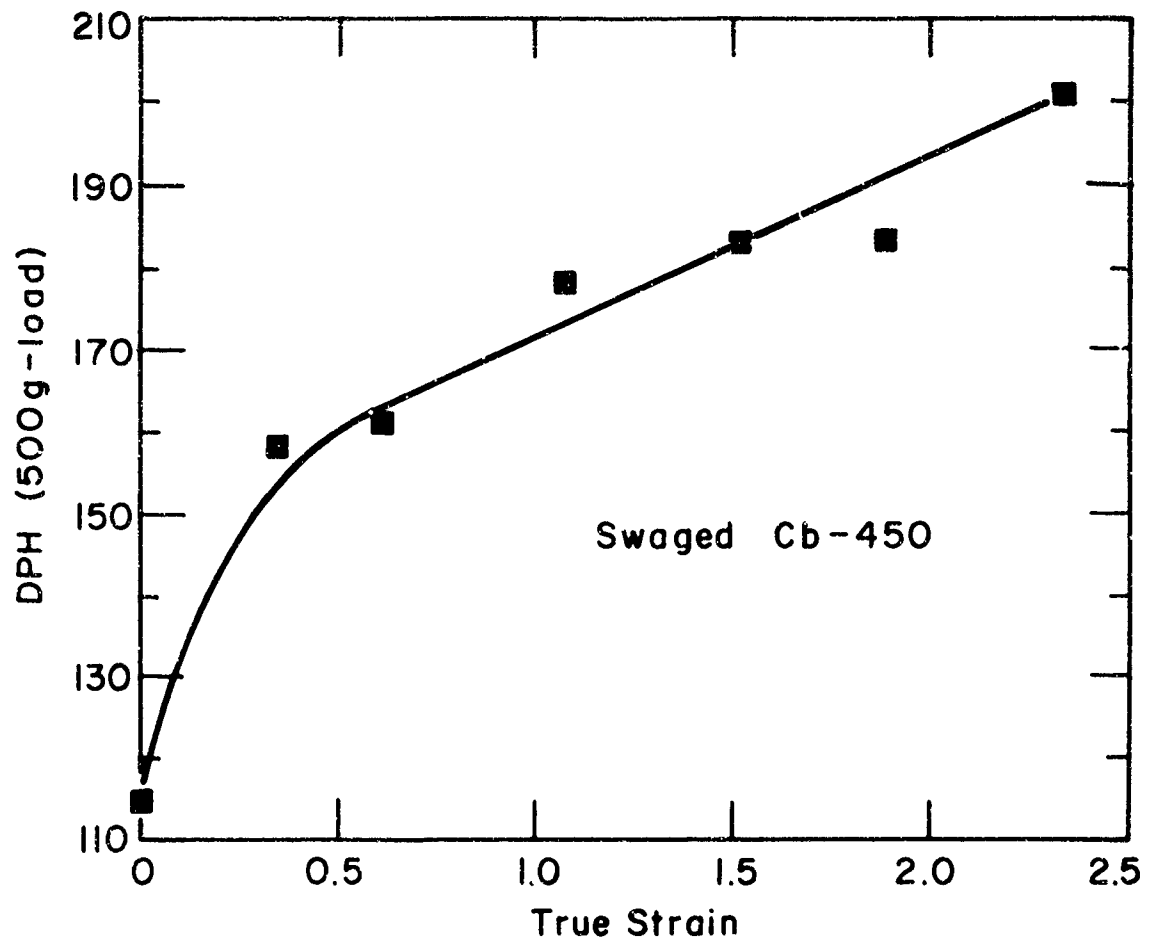
Fig. 6 Microhardness of swaged columbium

Crystal Axes Marked +
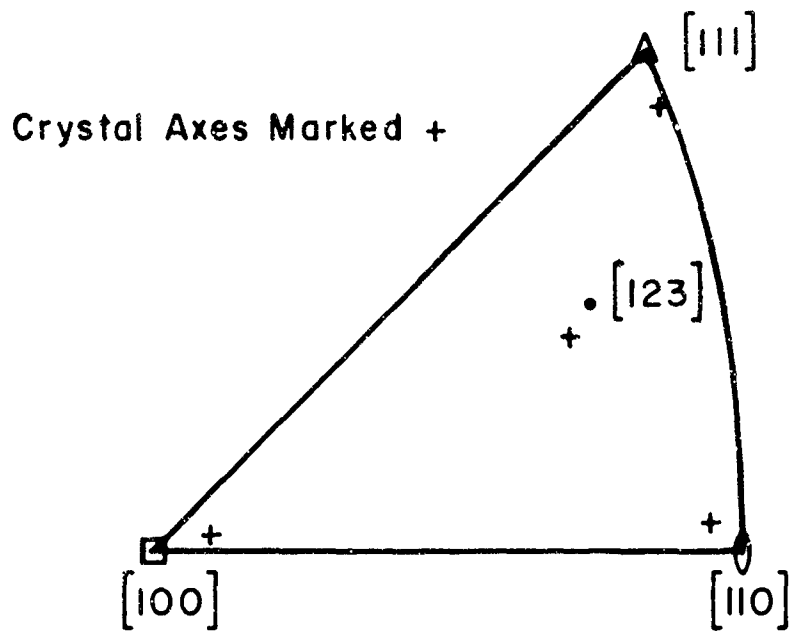
Fig. 7 Orientations of single crystals

20

(a) Thinning Apparatus
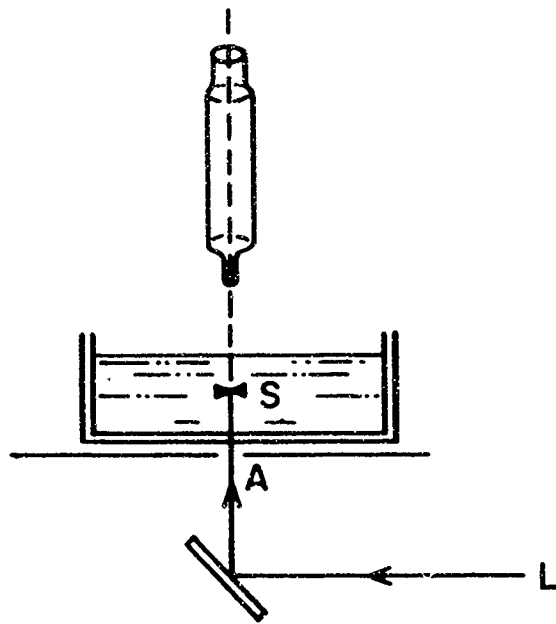
L – Light Source
A – Aperture
S – Specimen-Held in thinning bath by platinum clip.

(b) Thinning Sequence
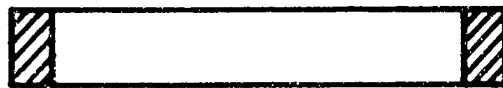
I. Edges of disc masked with lucite.
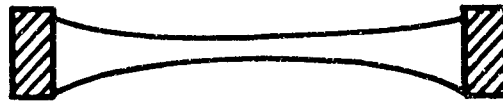
II. Thinning allowed to continue until a hole is seen using a microscope.
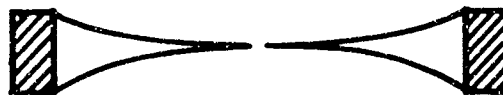
Fig. 8 Thin foil preparation technique
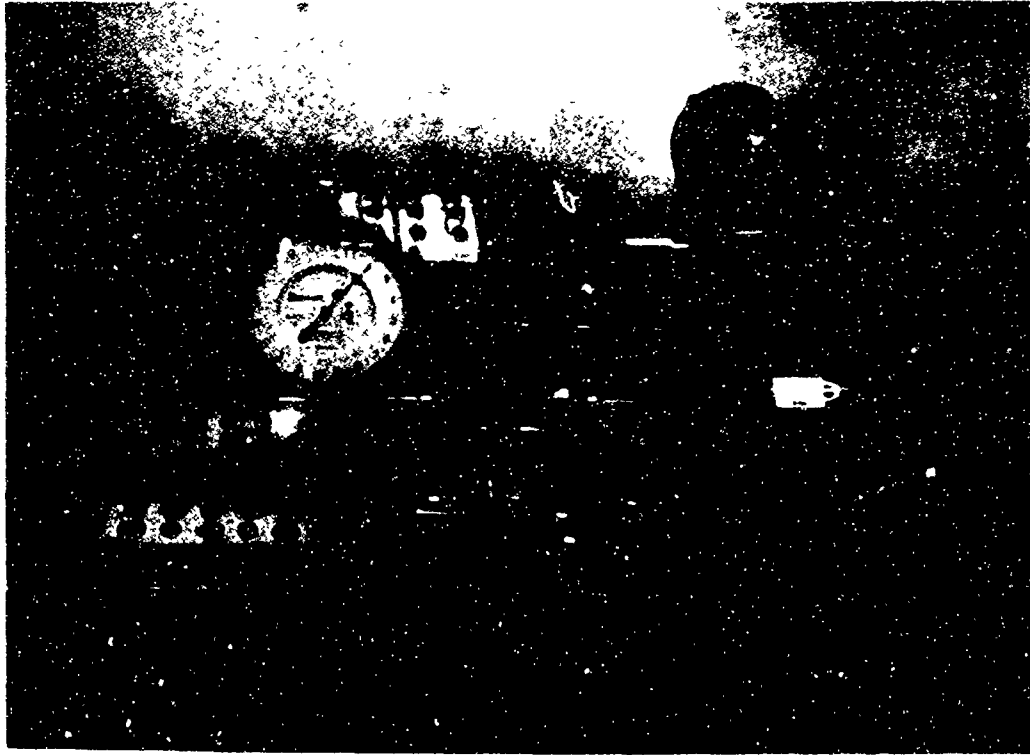
Fig. 9 Torsiometer

Fig. 10 Section of $[III]$ crystal, as received, X 40,000

Fig. II Section of $[123]$ crystal, as received, X40,000
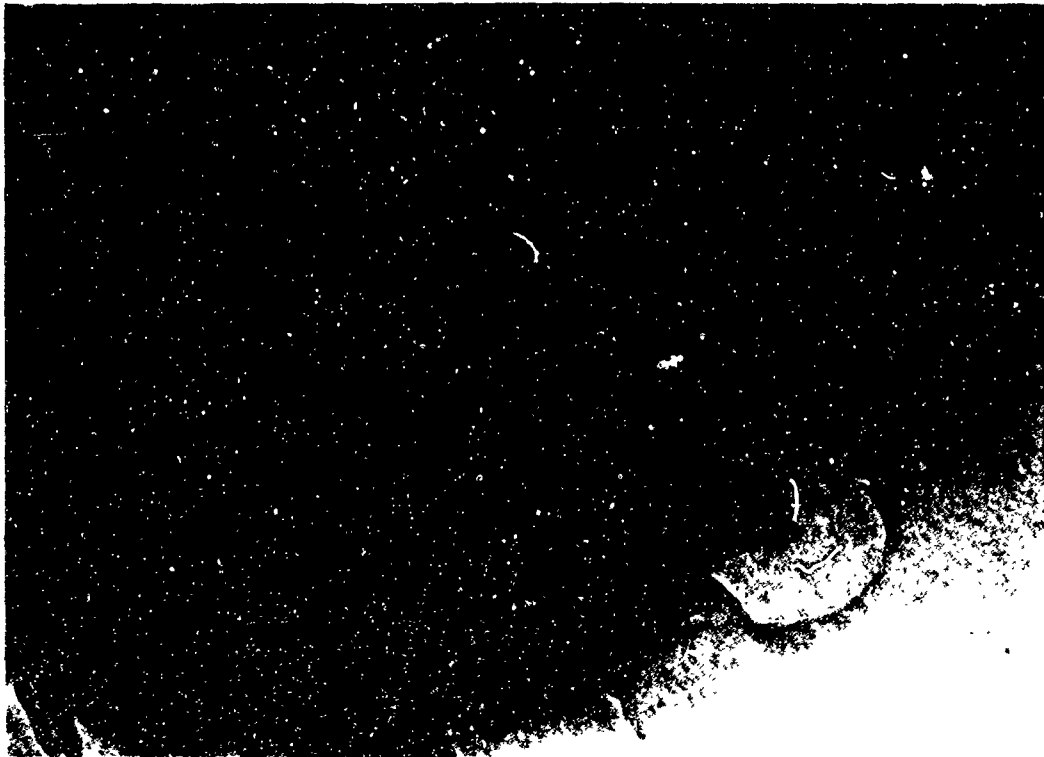
Fig. 12 Section of $[110]$ crystal, as received, X40,000
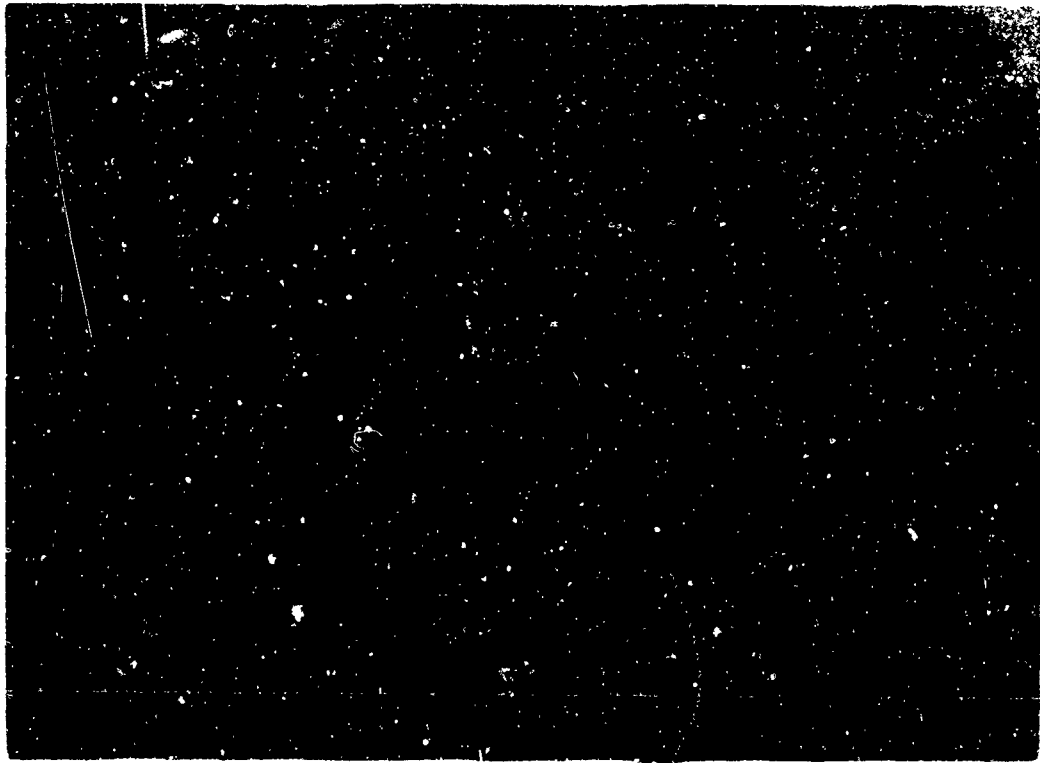
Fig. 13 Section of $[111]$ crystal, as received, X40,000
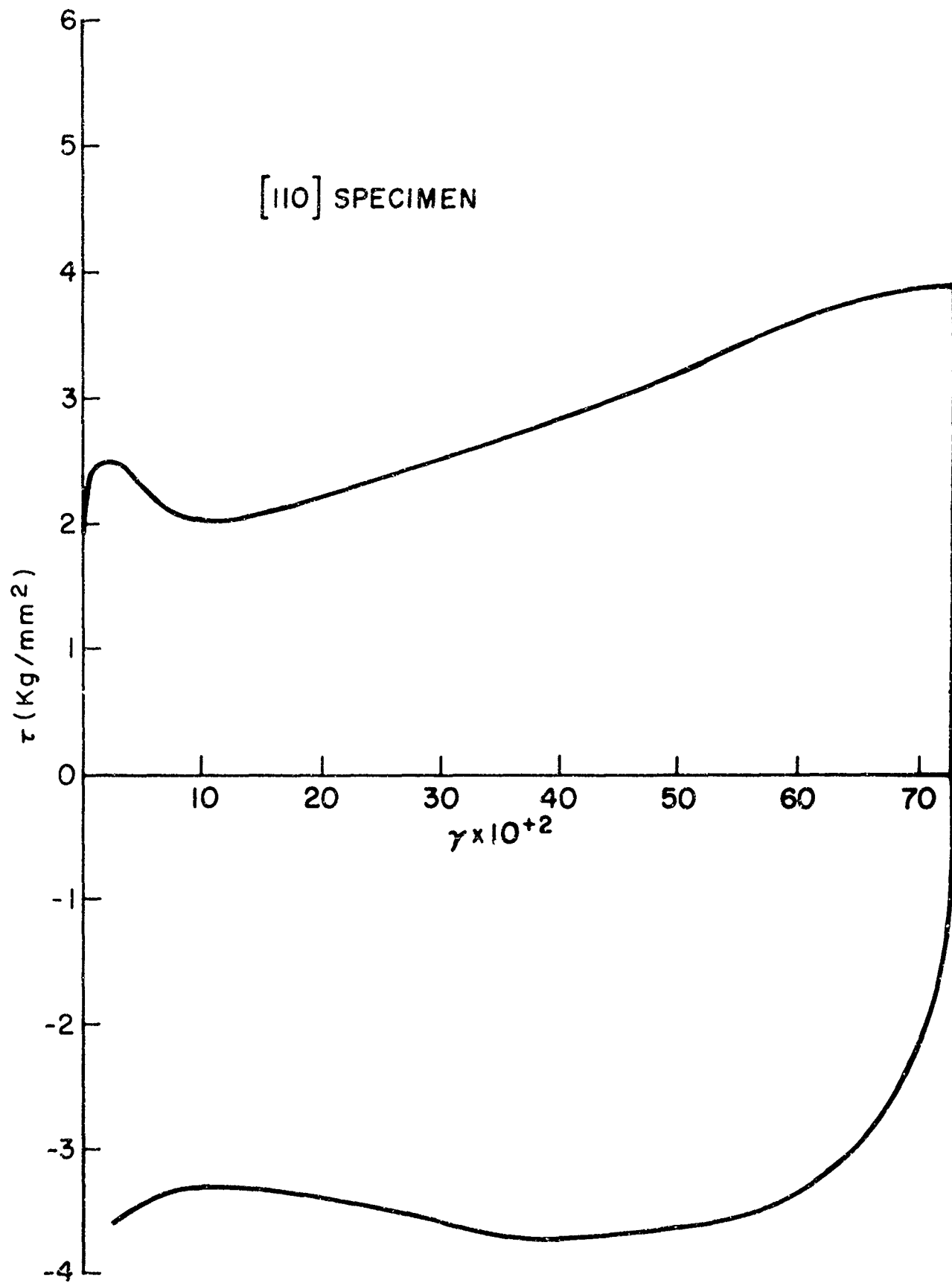
Fig. 14 Torque—twist curve, [110] crystal
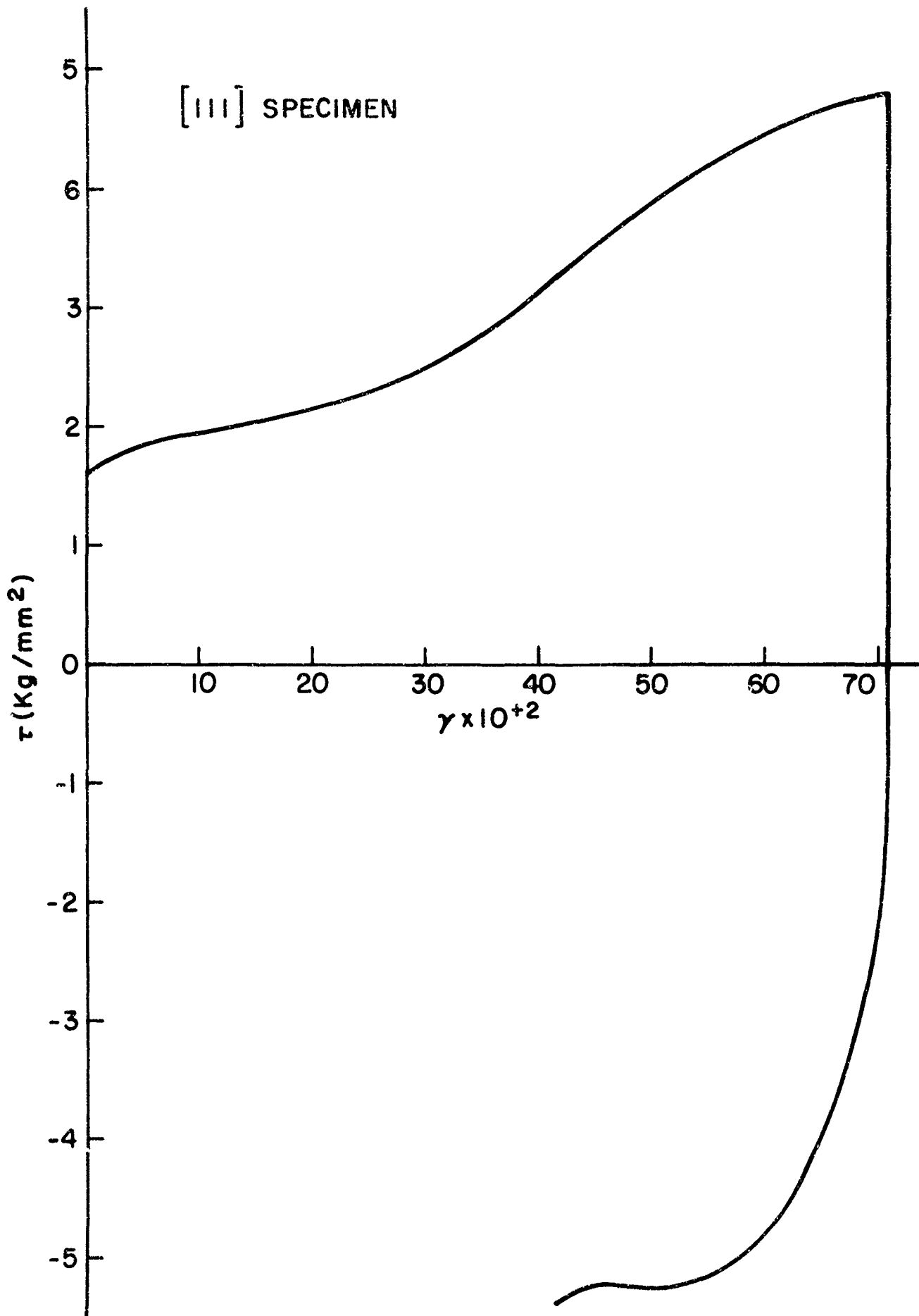
Fig. 15 Torque-twist curve, [111] crystal
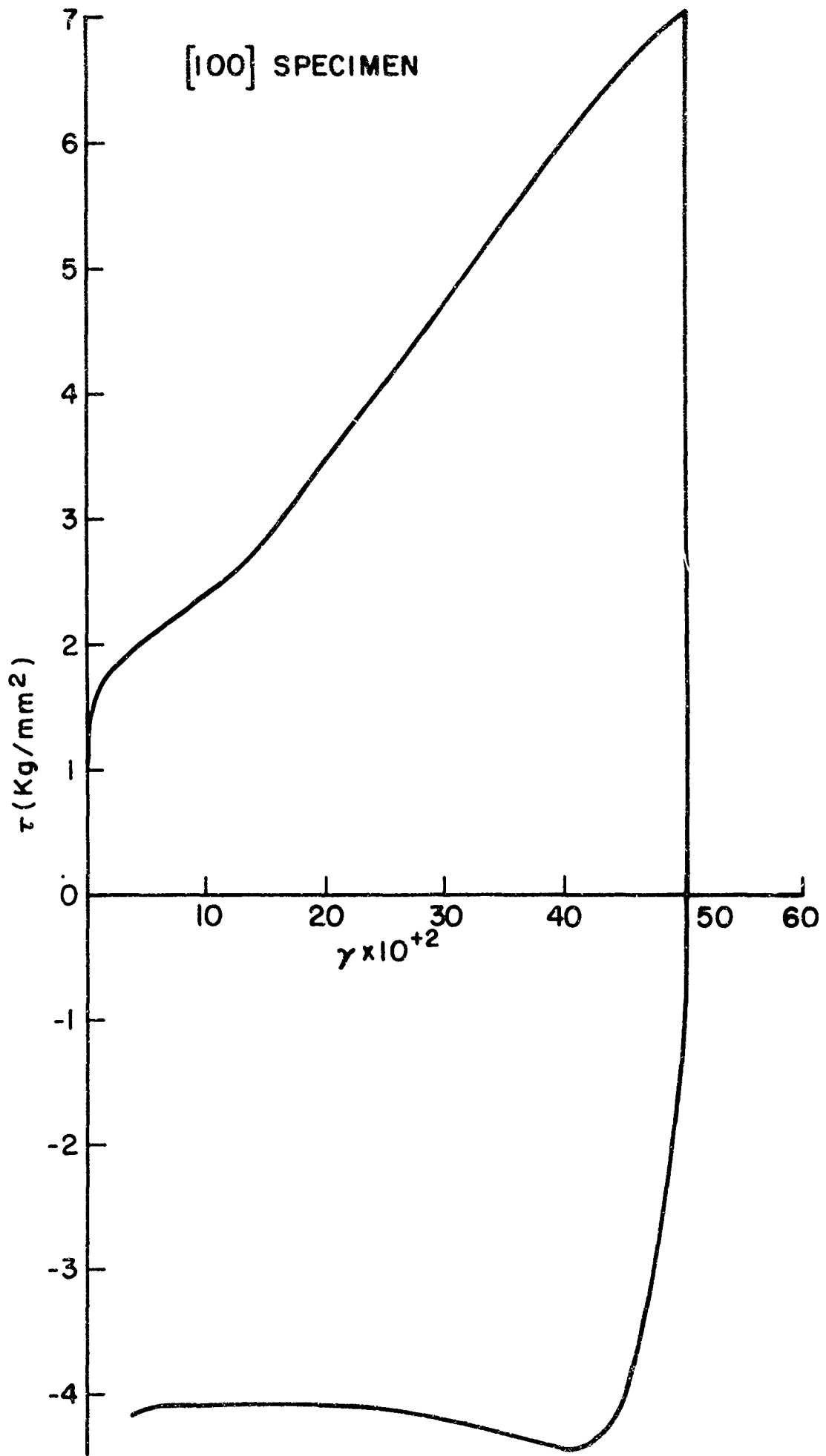
Fig. 16 Torque-twist curve, [100] crystal

27
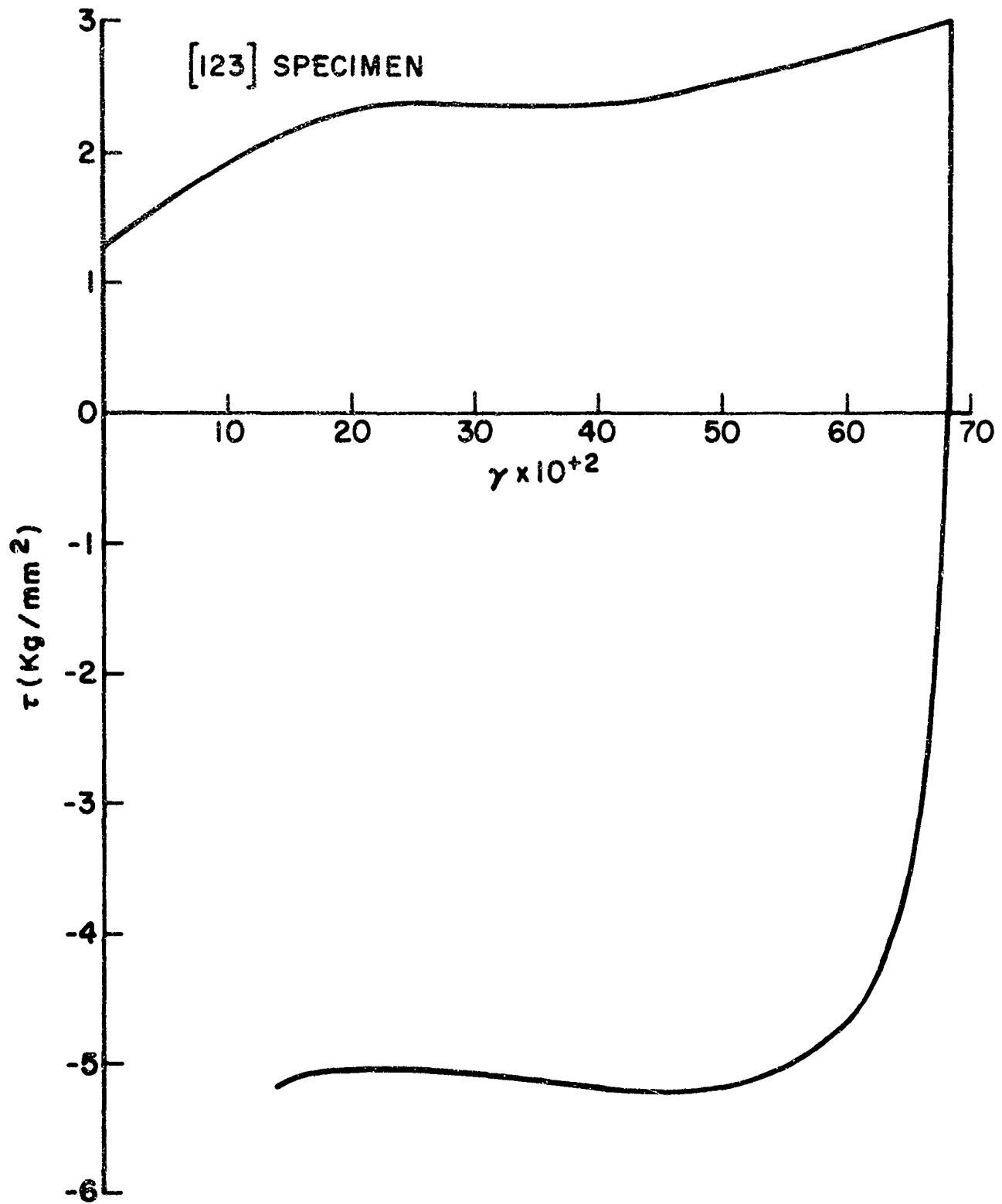
Fig. 17 Torque-twist curve, [123] crystal

28
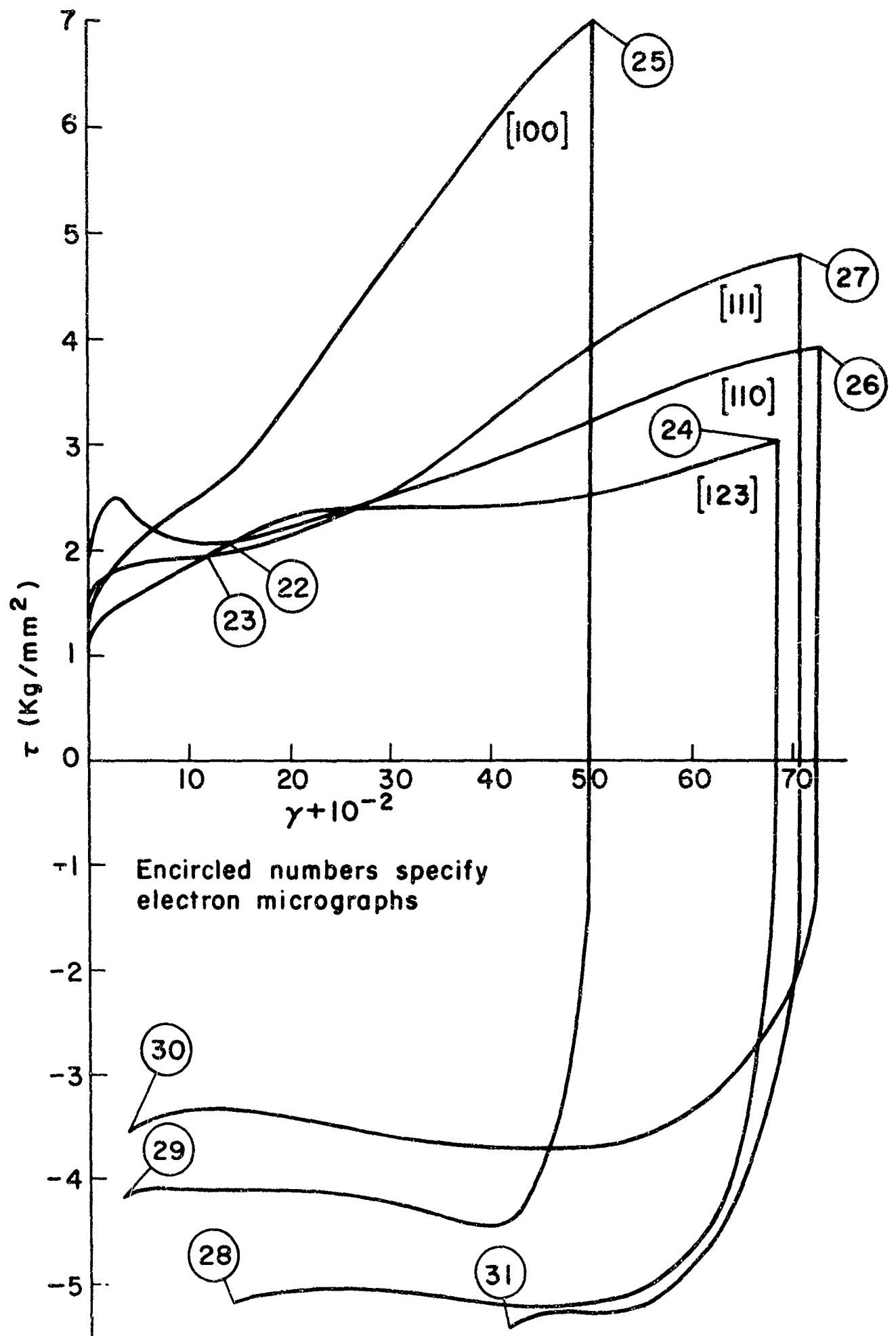
Fig. 18 Combined single crystal stress-strain curves
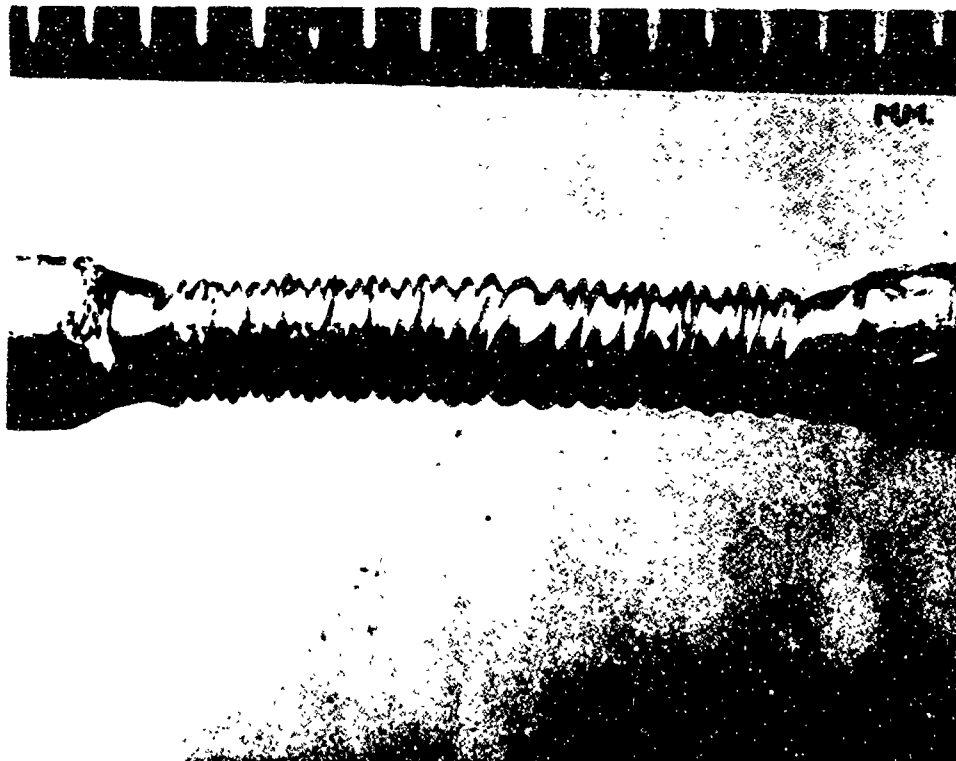
Fig. 19 $[123]$ crystal, appearance of surface after strain of 5.6

Fig. 20 Section of $[123]$ crystal, zero strain, X40,000

30
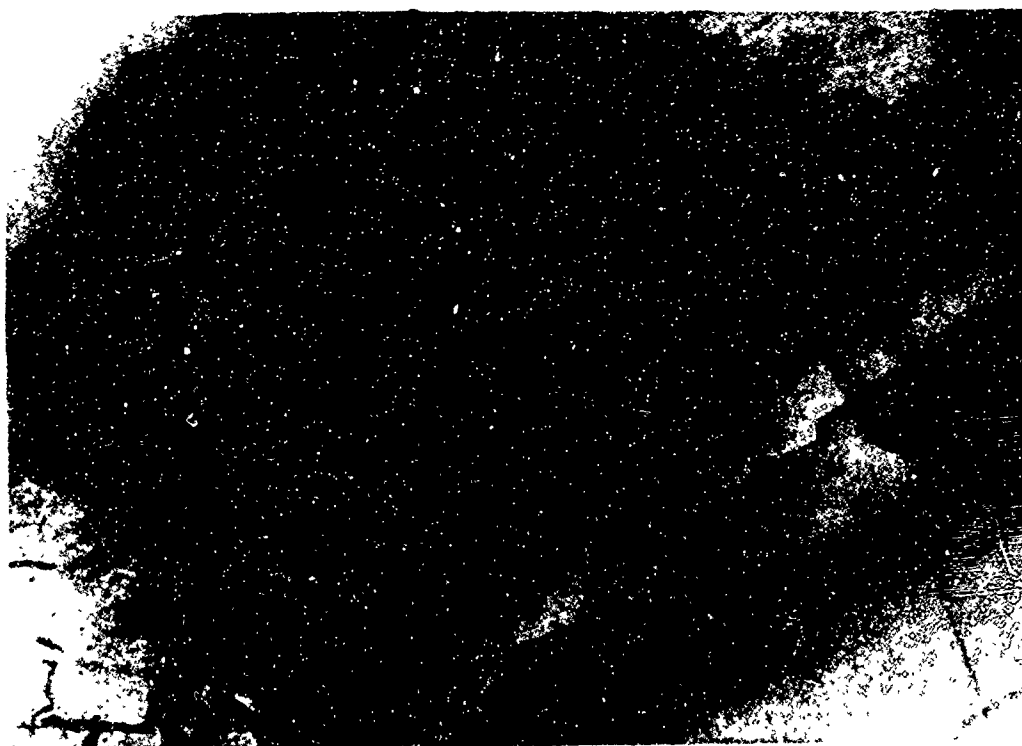
Fig. 21 Section of [100] crystal, zero strain, X40,000
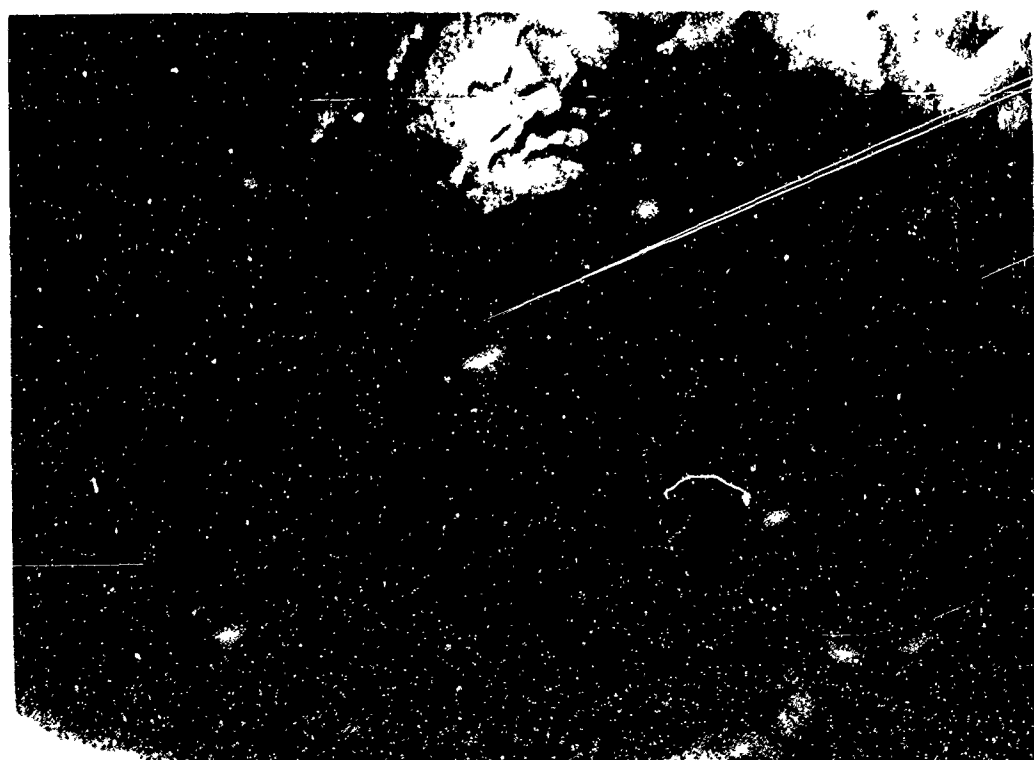
Fig. 22 Section of [110] crystal, strain of 0.14, X40,000

Fig. 23 Section of [III] crystal, strain 0.12, X40,000
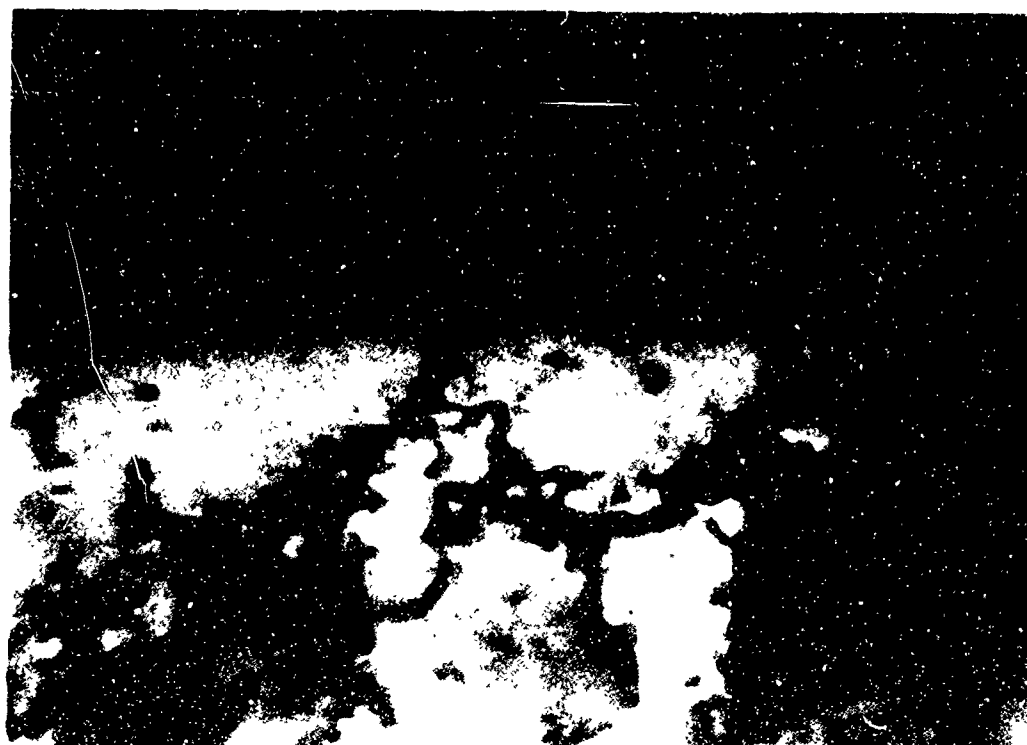
Fig. 24 Section of [123] crystal, strain of 0.685, X40,000
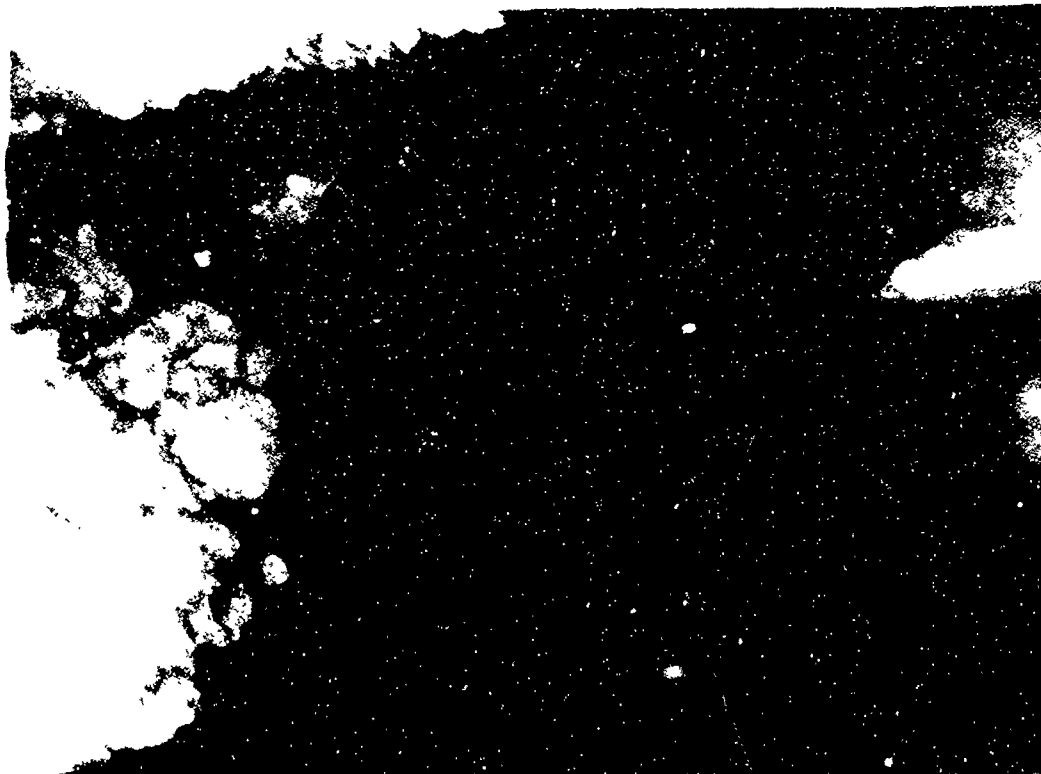
Fig. 25   Longitudinal section of $[100]$ crystal, strain of 0.50, X40,000
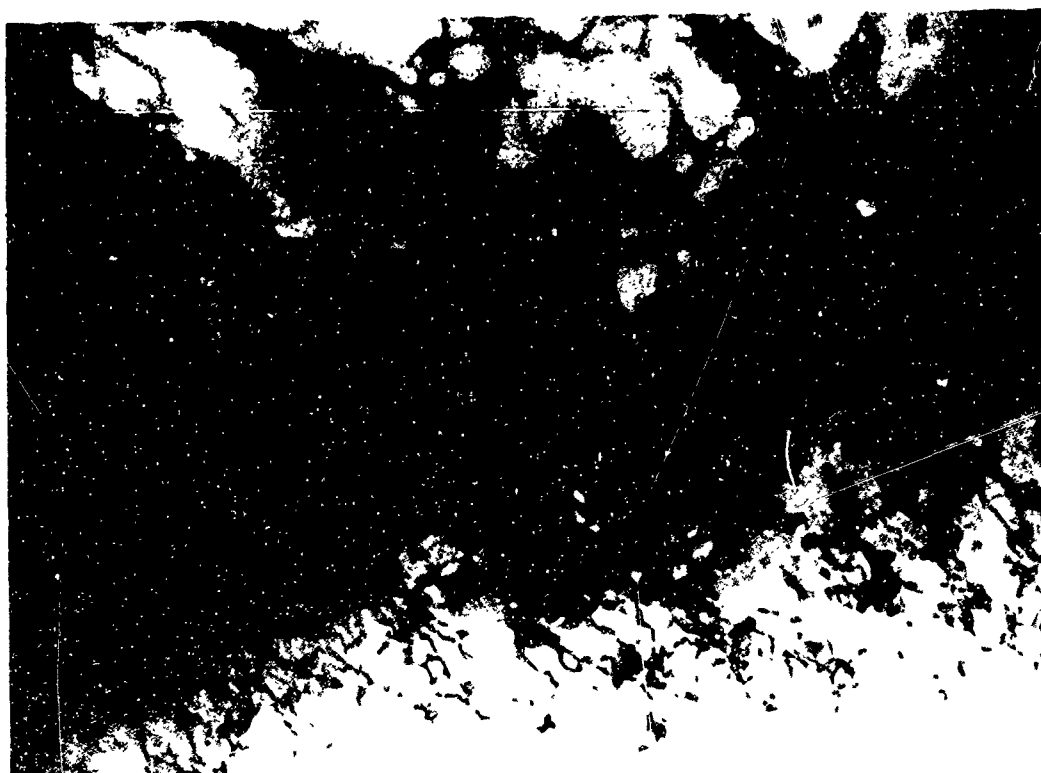
Fig. 26   Section of $[110]$ crystal, strain of 0.72, X40,000

Fig. 27 Section of [III] crystal, strain of 0.71,X40,000
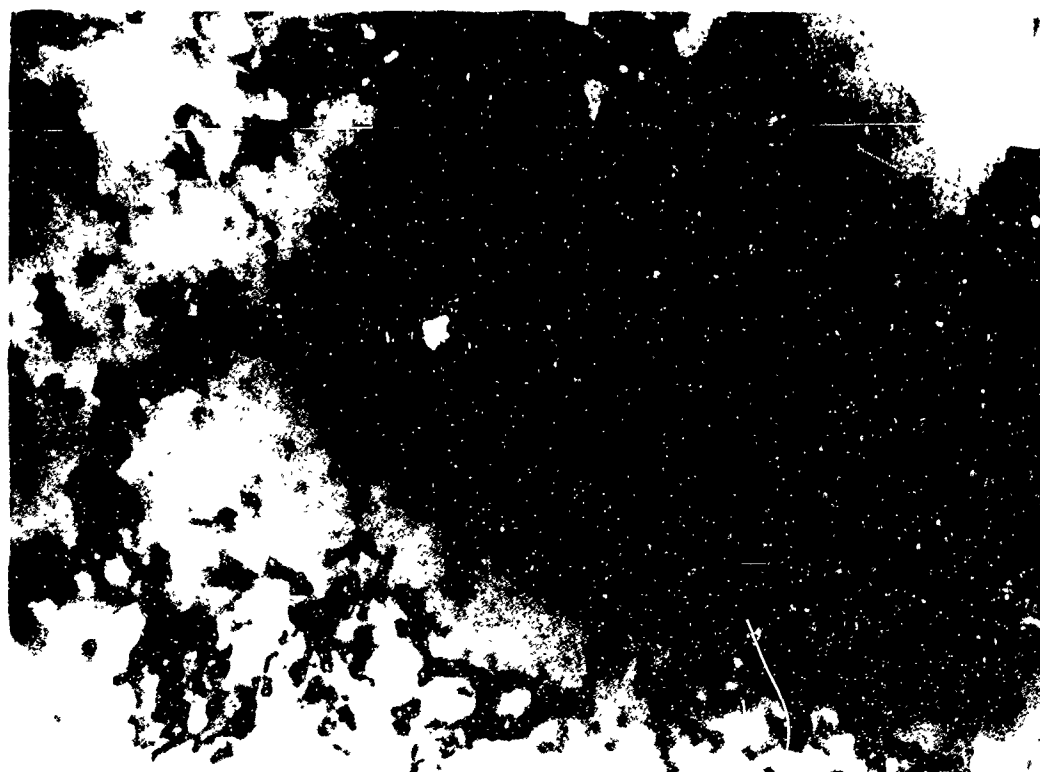
Fig. 28 Section of [123] crystal, strain of +0.685 −0.545, X40,000
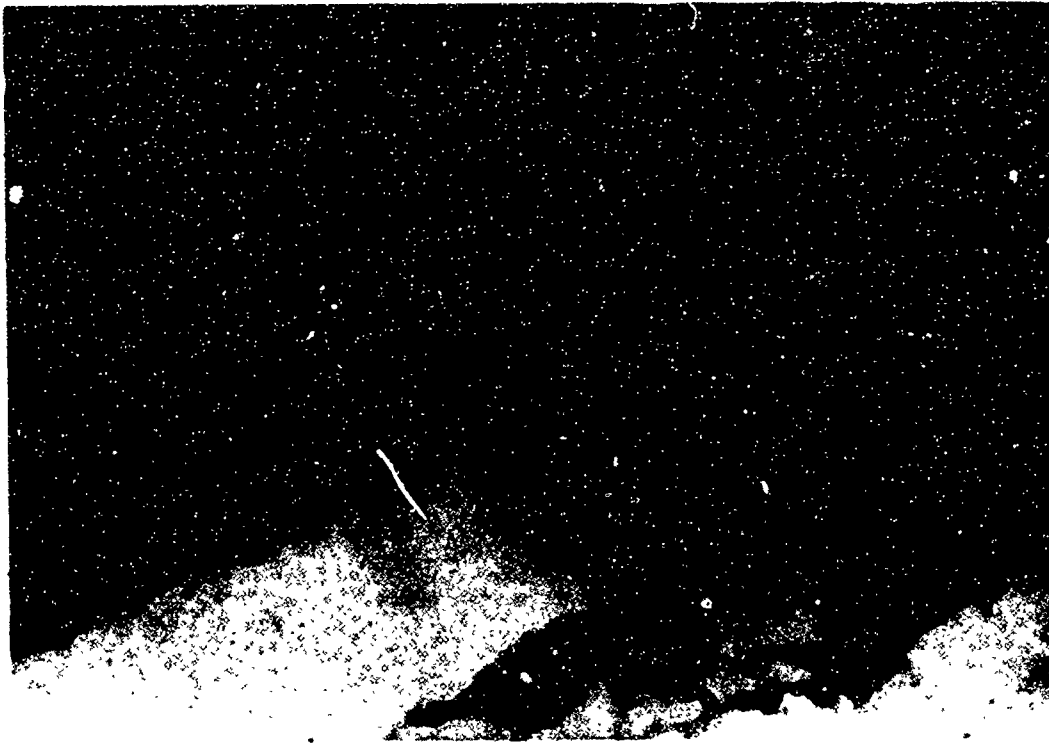
Fig. 29 Longitudinal section of [100] crystal, strain of +0.50 -0.47, X40,000
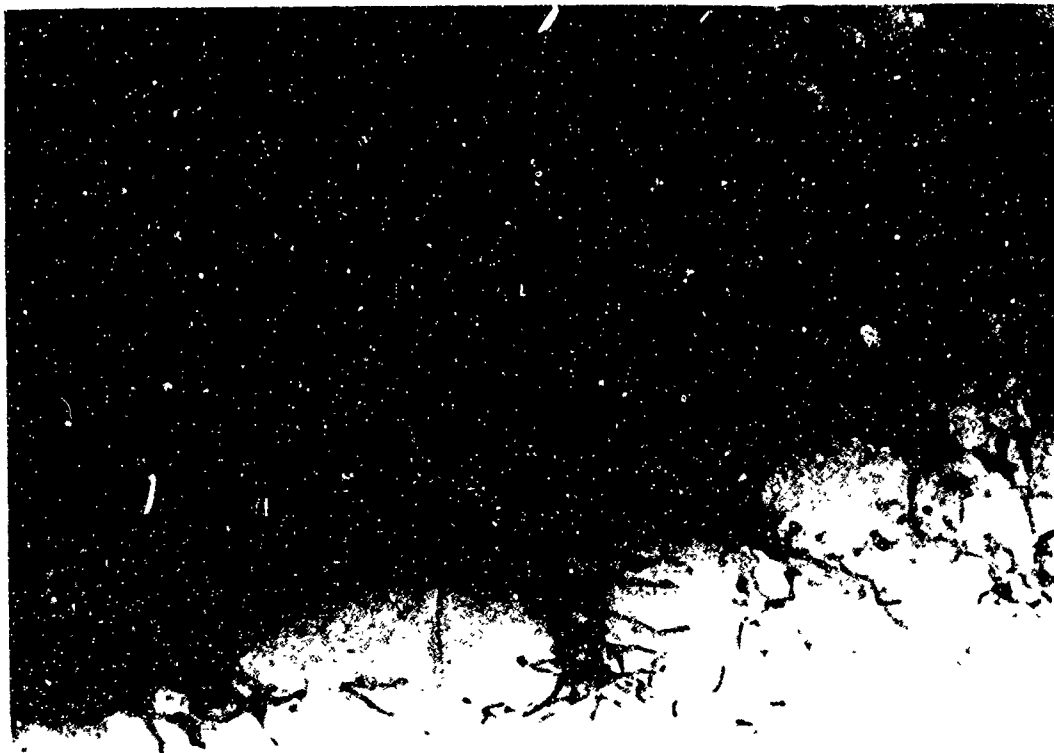
Fig. 30 Section of [110] crystal, strain of +0.72 -0.69, X40,000
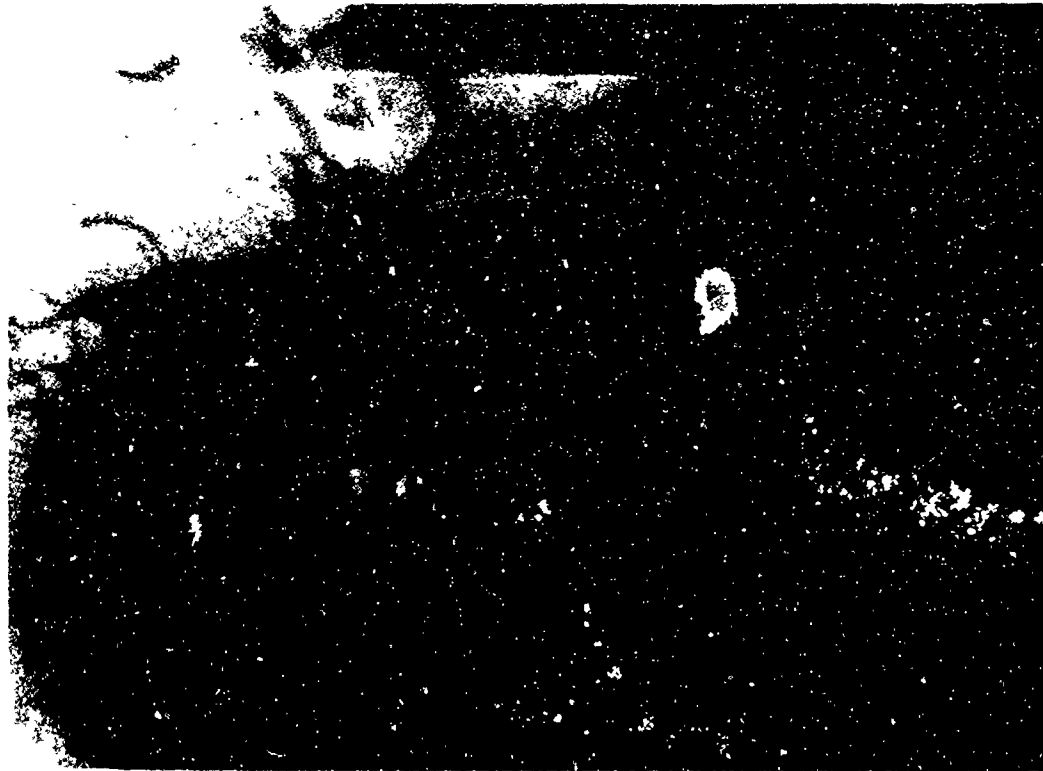
Fig. 31 Section of $[111]$ crystal, strain of +0.71 -0.295, X40,000
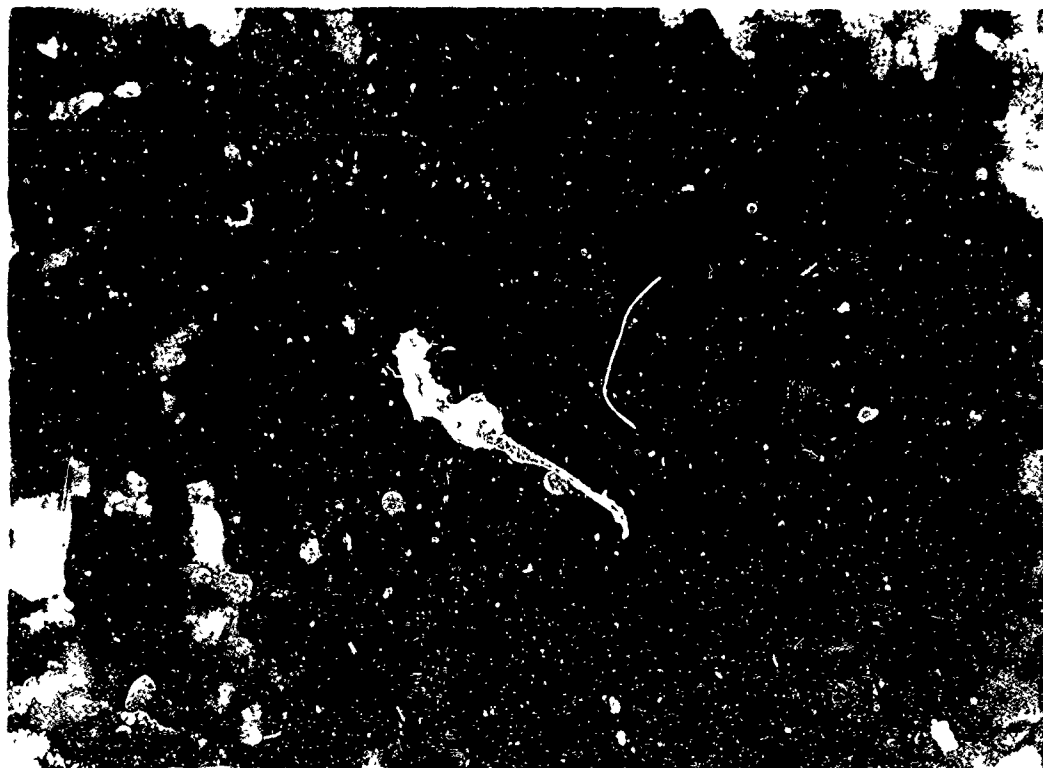
Fig. 32 Section of drawn wire, X40,000
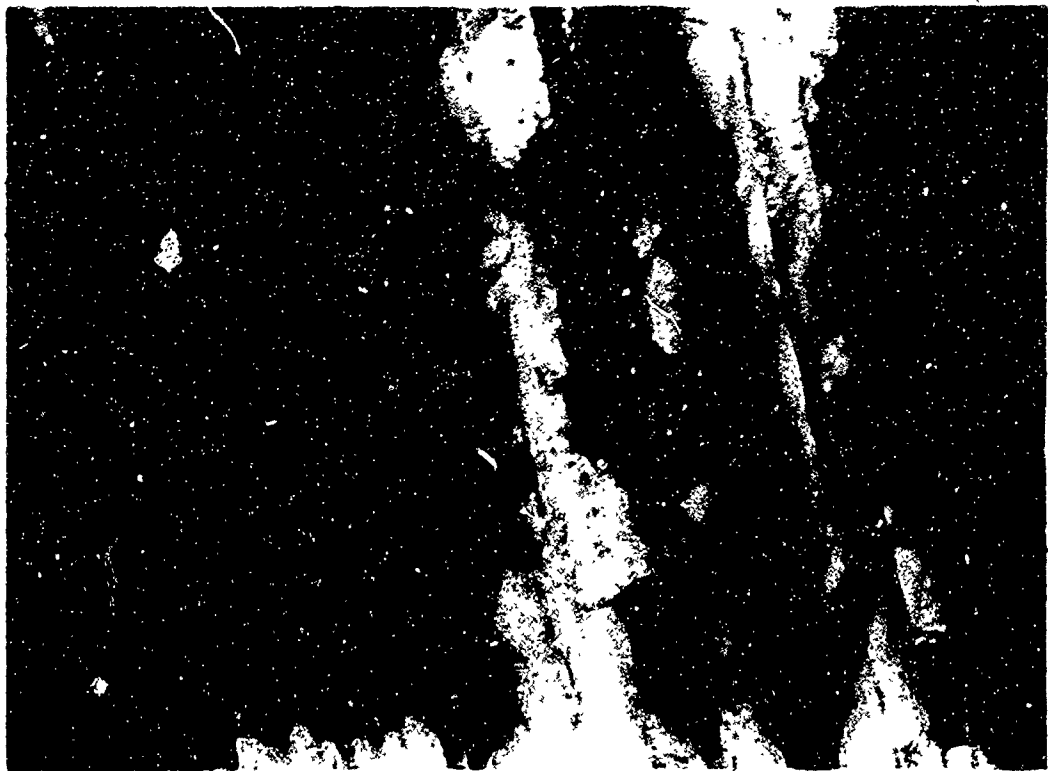
Fig. 33 Longitudinal section of drawn wire, X40,000
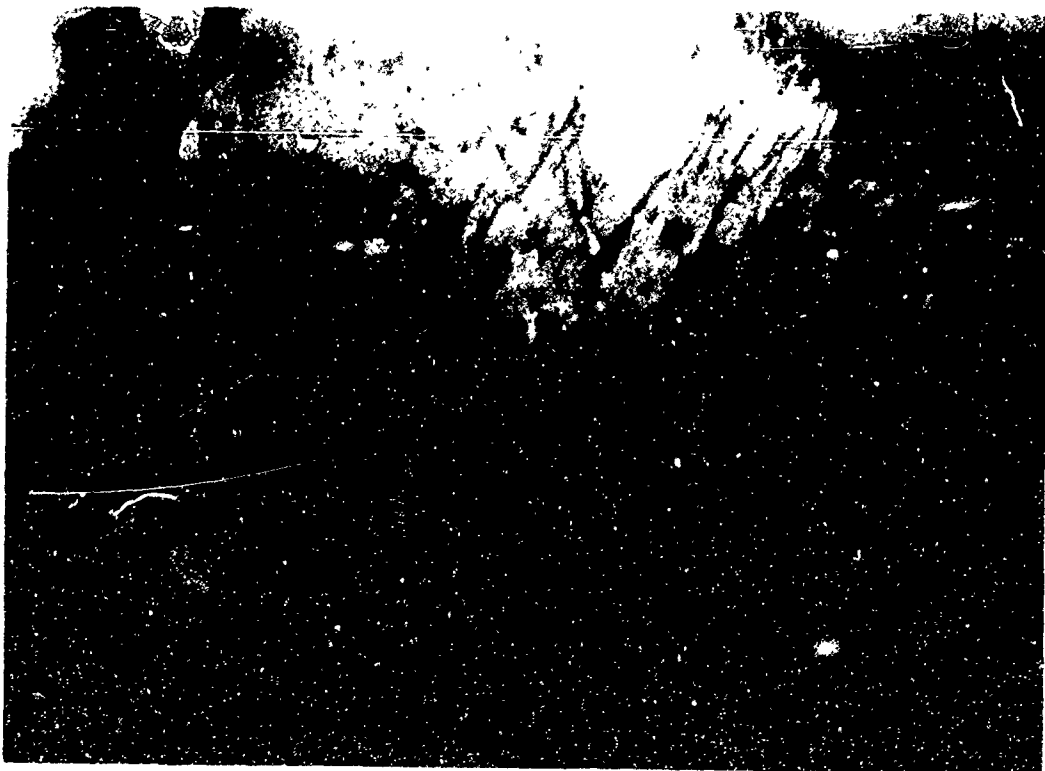
Fig. 34 Drawn wire annealed at 900°C, X40,000
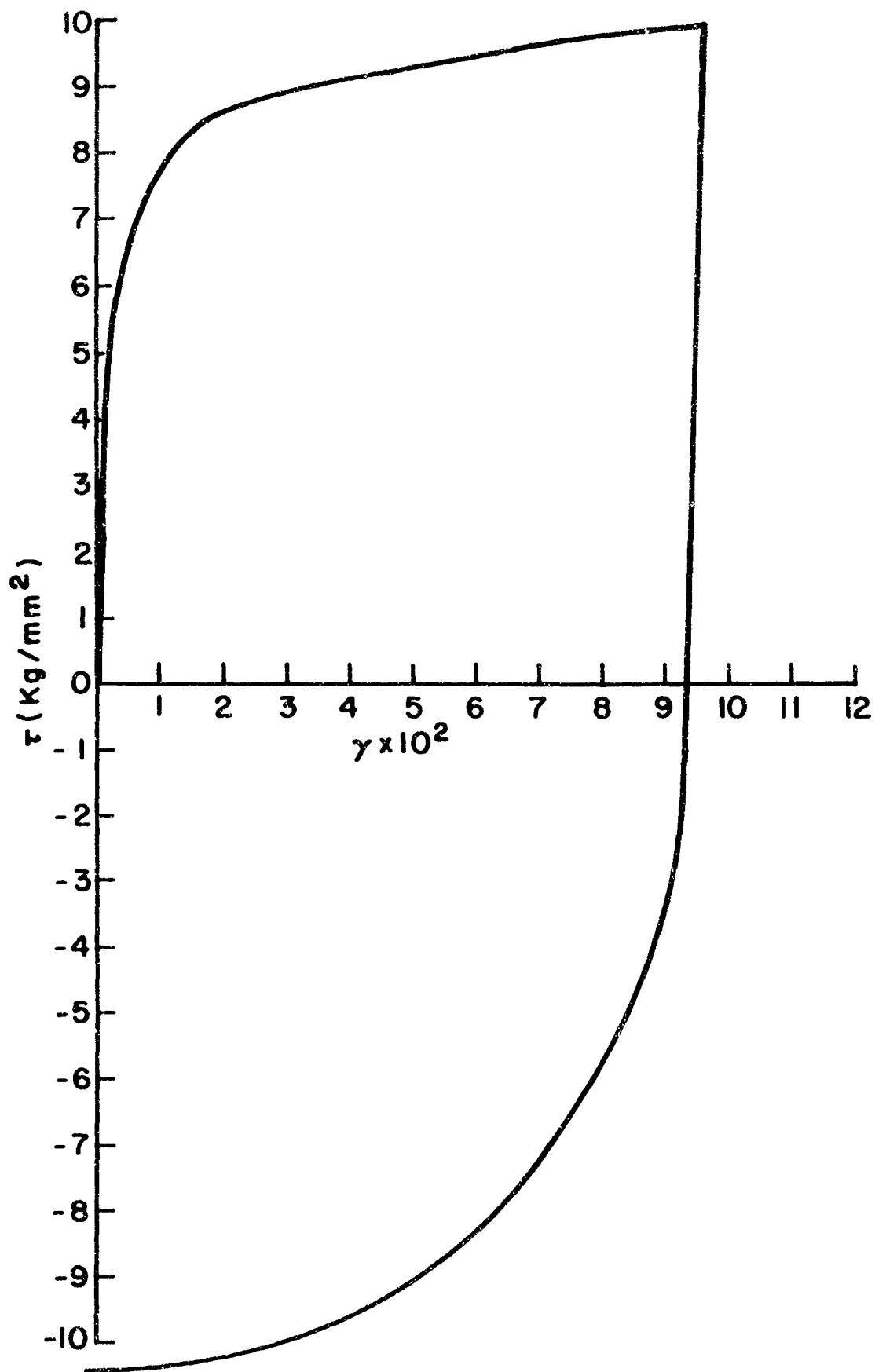
Fig. 35 Torque-twist curve of drawn wire,
reversal after forward strain of 0.092
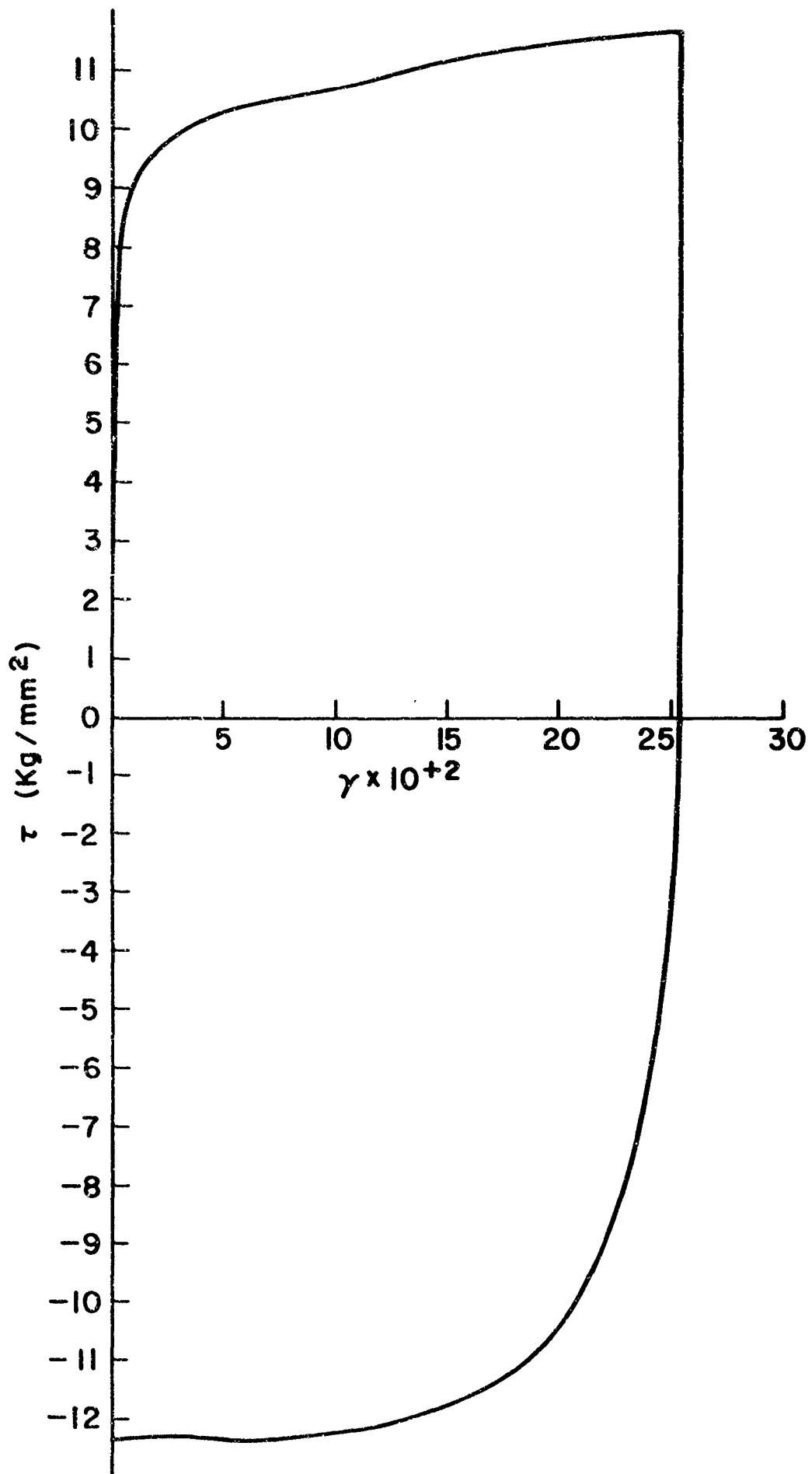
Fig. 36 Torque - twist curve of drawn wire,
reversal after forward strain of 0.26

39
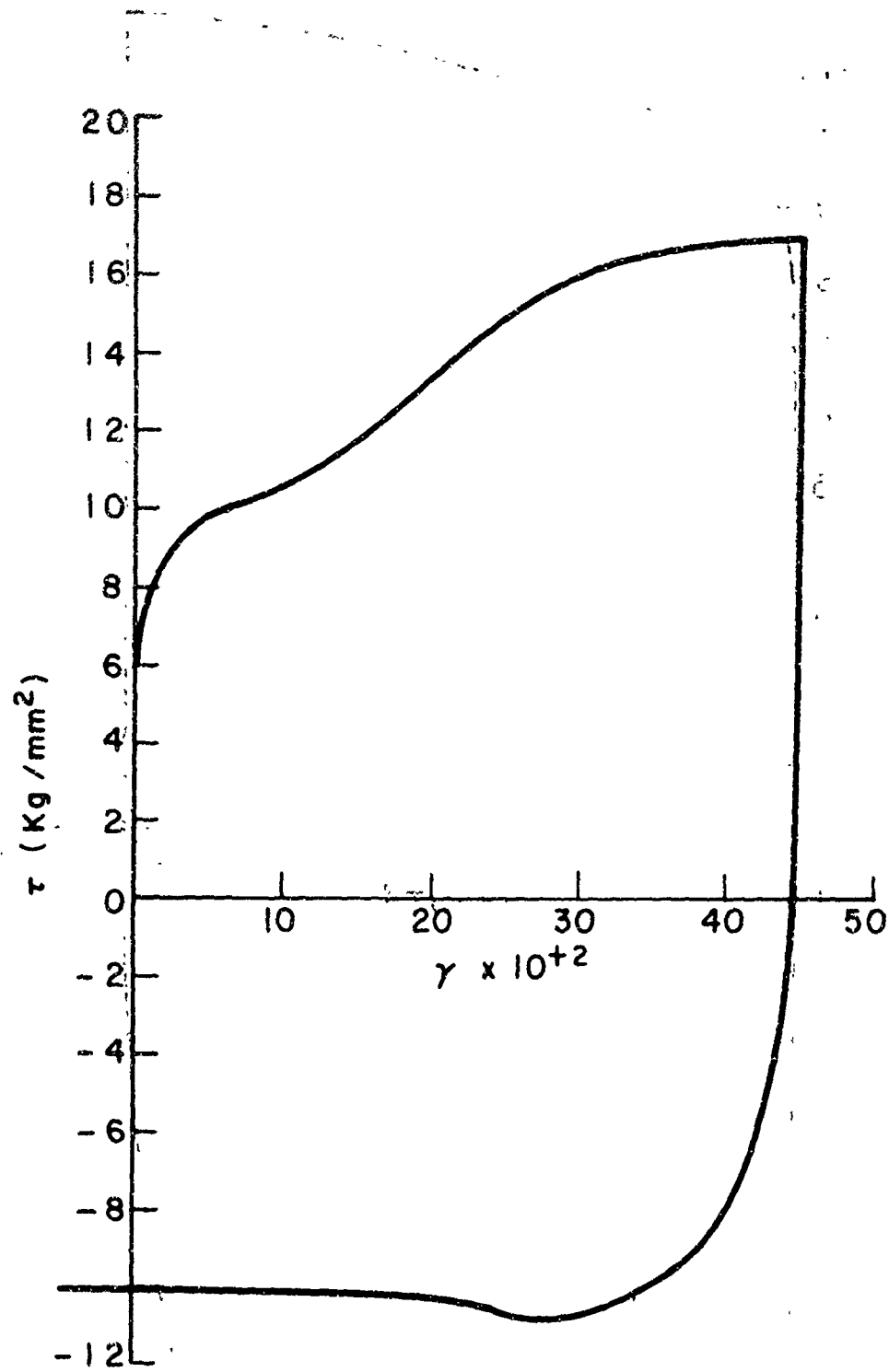
Fig. 37 Torque–twist curve of drawn wire,
reversal after forward strain of 0.45
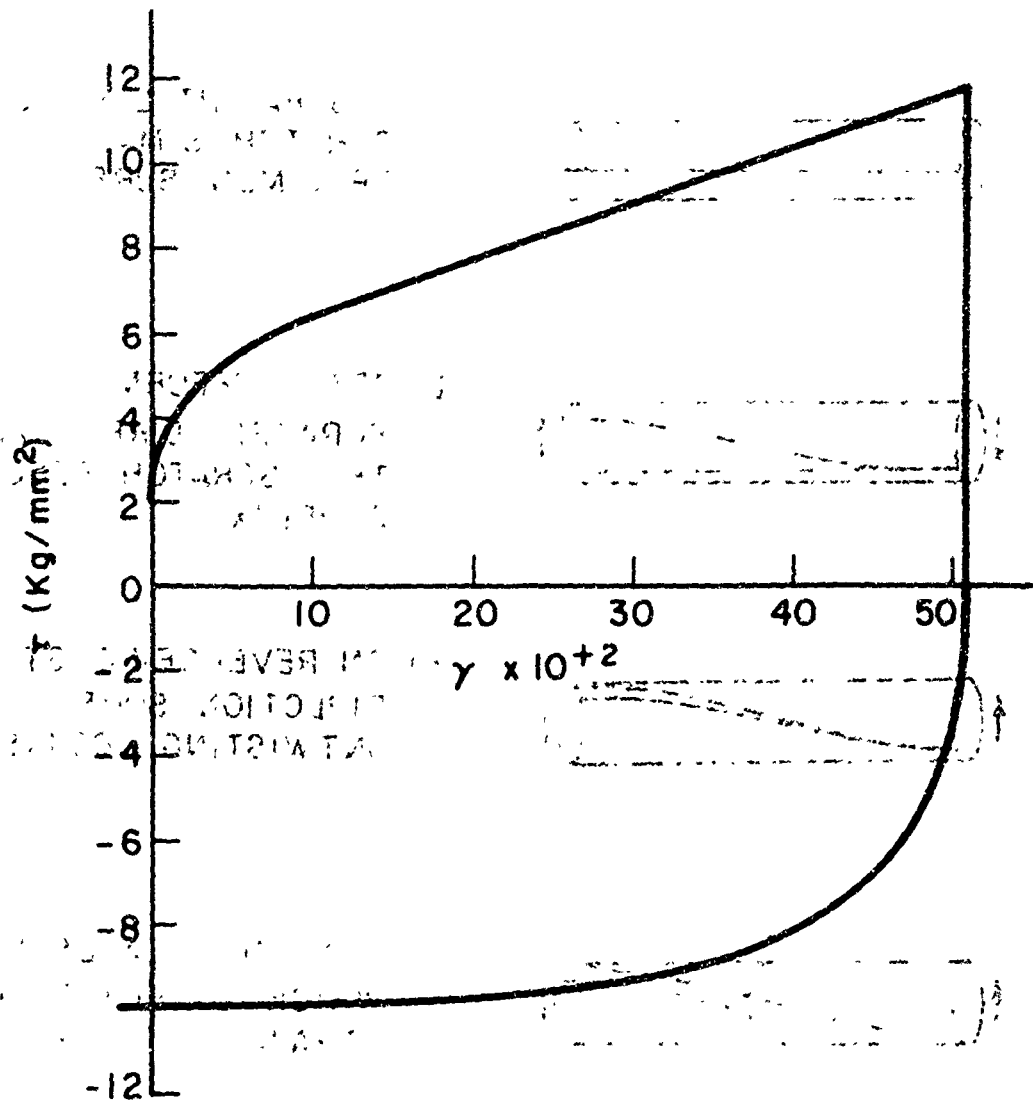
Fig. 38 Torque-twist curve of annealed wire,
reversal after forward strain of 0.51
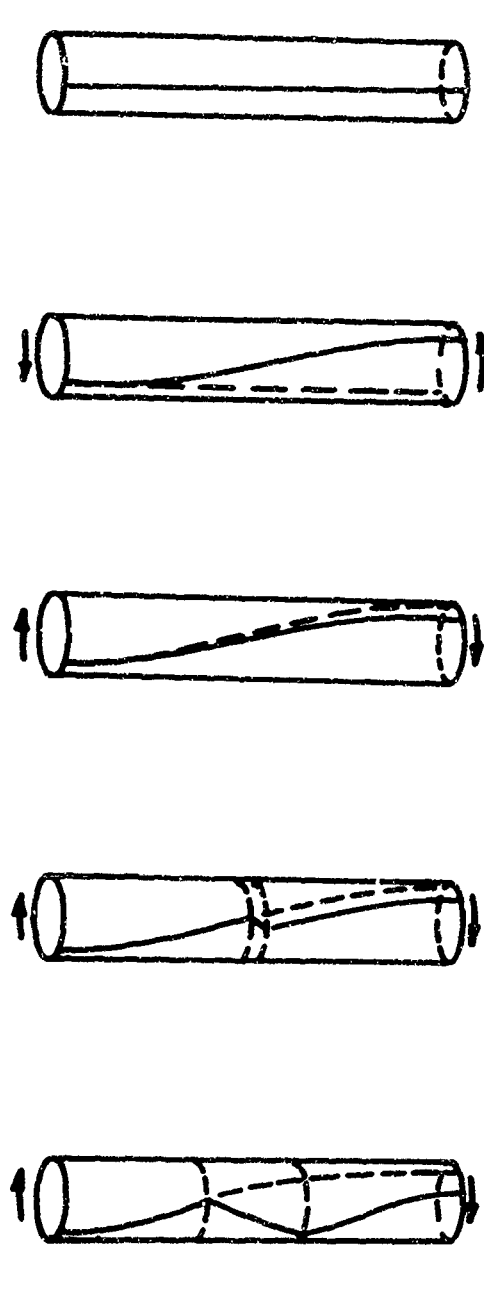
a) A STRAIGHT LONGITUDINAL
SCRATCH IS MADE ON THE
SPECIMEN SURFACE

b) AFTER DEFORMATION IN
"FORWARD" DIRECTION
THIS SCRATCH BECOMES
A HELIX

c) ON REVERSEING STRESS
DIRECTION SOME UNIFORM
UNTWISTING OCCURS

d) BAND NUCLEATES WITHIN
WHICH DIRECTION OF
STRAIN IS REVERSED

e) CONTINUED STRAINING
OCCURS BY PROPAGATION
OF THIS BAND THROUGH
THE GAGE LENGTH

Fig. 39 Band formation in drawn wire

42

Fig. 40 Appearance of band on wire specimen
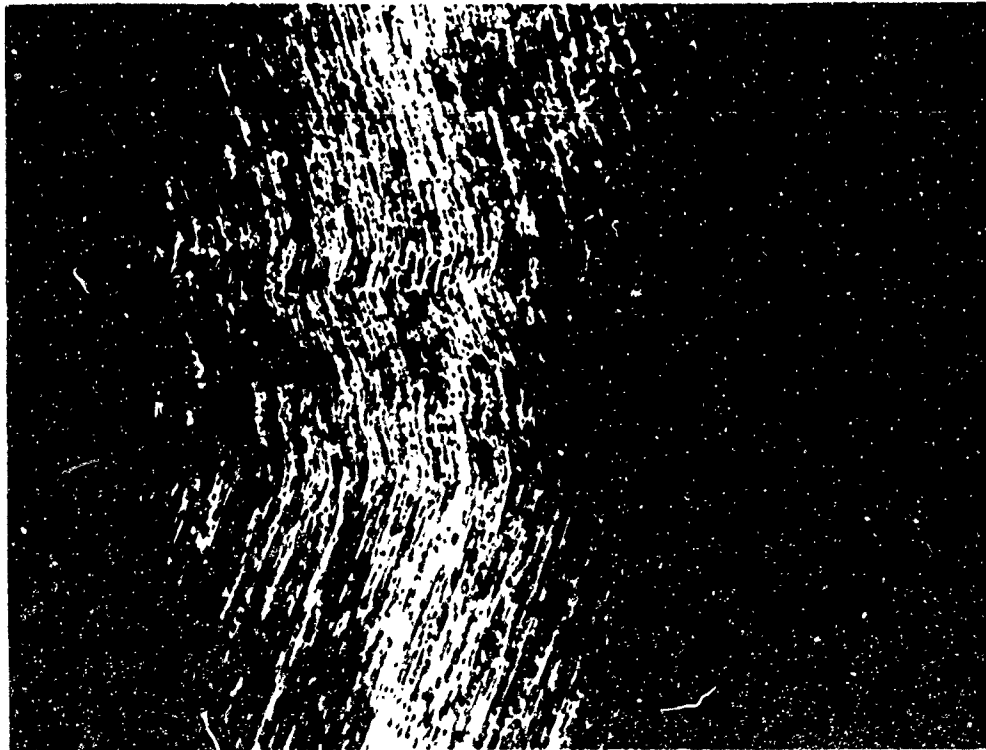
Fig. 41 Appearance of band front, X200
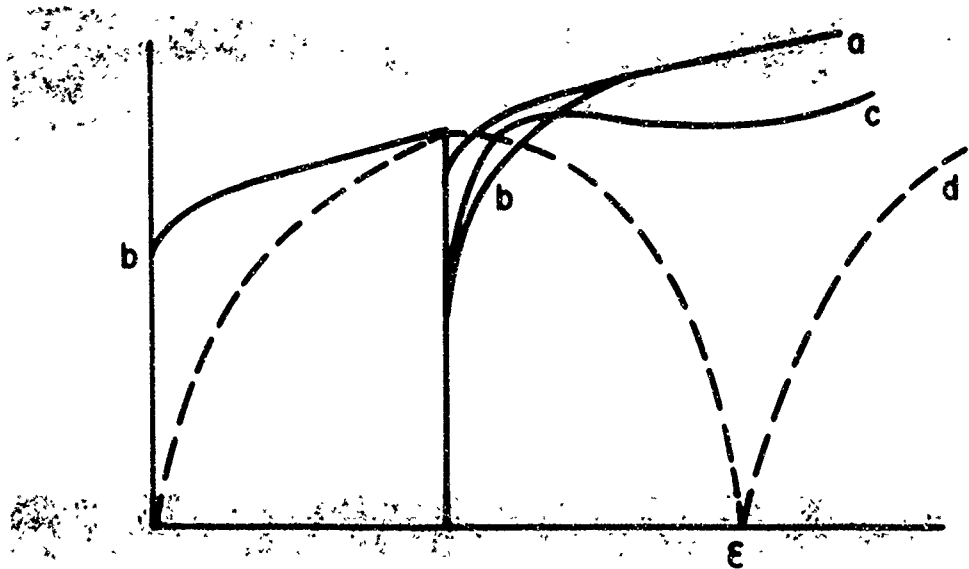
a) CONTINUED FORWARD STRAINING

b) CLASSICAL BAUSCHINGER EFFECT
ON REVERSED STRAINING

c) TYPICAL RESULT FOR SINGLE CRYSTALS
OR COLD WORKED POLYCRYSTALS IN
THIS INVESTIGATION

d) BEHAVIOUR OF TAYLOR MODEL ON
REVERSED STRAINING

Fig. 42 Qualitative stress-strain behavior

CELL WALL   CELL INTERIOR
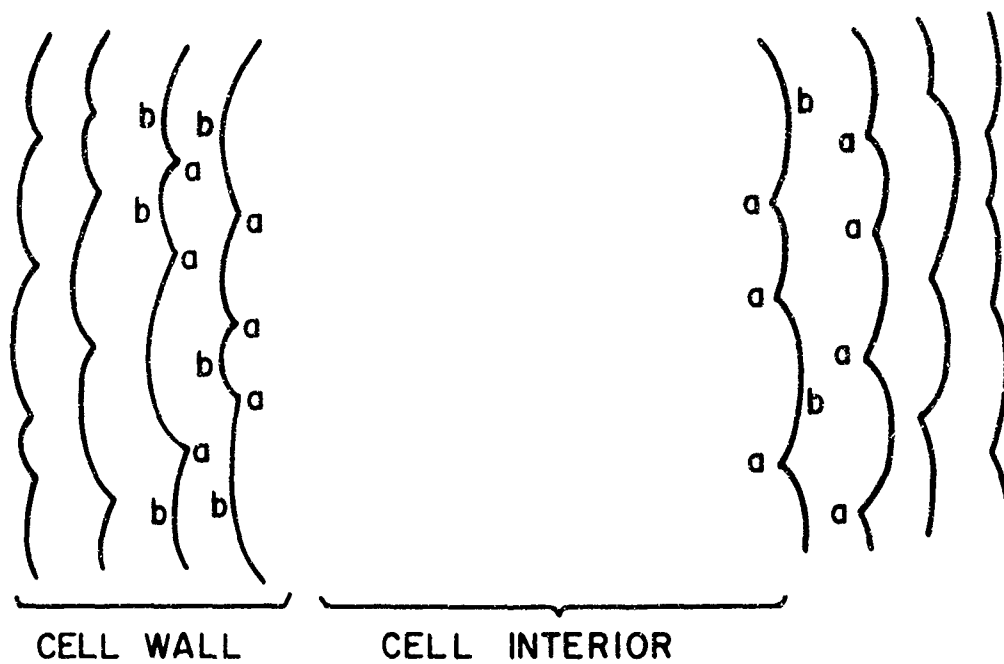
a - VACANCY JOGS PRODUCED DURING
    FORWARD STRAINING

b - INTERSTITIAL JOGS

Fig. 43 Cell wall model